EFFECTS OF MATERNAL IMMUNIZATION AGAINST MYOSTATIN ON SKELETAL MUSCLE MASS OF OFFSPRING IN MICE

A THESIS SUBMITTED TO THE GRADUATE DIVISION OF THE UNIVERSITY OF HAWAI'I IN PARTIAL FULFILLMENT OF THE REQUIREMENTS FOR THE DEGREE OF

MASTER OF SCIENCE

IN

ANIMAL SCIENCES

MAY 2007

By

Naveen K. Bobbili

Thesis Committee:

Yong-Soo Kim, Chairperson
Jinzeng Yang
Michael A. Dunn

We certify that we have read this thesis and that, in our opinion, it is satisfactory in scope and quality as a thesis for the degree of Master of Science in Animal Sciences.

THESIS COMMITTEE

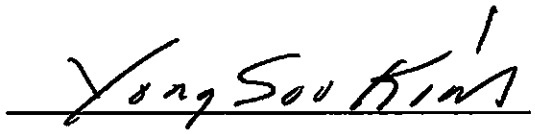

(Chairperson)

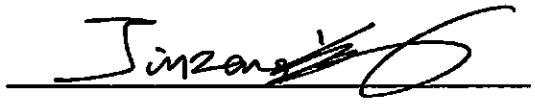

ACKNOWLEDGMENT

Having received help from so many people, it is hard to include everyone, but there are several individuals without whom, I could not have made it this far. First, I would like to thank my advisor, Dr. Yong-Soo Kim, whose constant guidance, support and encouragement helped me get the most out of my Master's program. Dr. Kim recognized my potential and helped in every possible way to hone my skills. I am grateful to Dr. Kim for giving me the opportunity to work on a couple of different projects and for including me as a co-author in a couple of publications. I would also like to thank my thesis committee members, Dr. Jinzeng Yang and Dr. Michael Dunn, for their keen review, advice and constructive comments. Dr. Yang and Dr. Dunn also played crucial roles in my learning process as they provided their academic expertise and laboratory resources. I thank Mrs. Cory S. Tauyan, for training and help in carrying out chicken project and Baoping Zhao for training in the transgenic mice project. Working with my colleagues, especially Allison, Kyle and Kyung-Ho had always been fun for they made the circumstances in the lab pleasant to work in.

I would like to thank my mom for her constant support, encouragement and prayers. Friends, including Kyle, Nicole and Simon provided great moral support and companionship. Finally, I thank my friend Ravi Putluru for what he has done to help me rediscover myself. My special thanks go to Dr. Chin Lee for his help in my personal and professional pursuits. It is acknowledged that the United State Department of Agriculture (USDA) T-STAR program supported this project.

ABSTRACT

Myostatin (growth & differentiation factor-8), a member of the transforming growth factor-β superfamily, is a potent negative regulator of skeletal muscle growth. Previous studies have demonstrated hypermuscularity being induced by the absence or suppression of functional myostatin and conversely, muscle atrophy upon myostatin overexpression or administration. These studies indicate that myostatin-blockade has potential applications in improving muscle mass in farm animals and in treating muscle atrophies in humans. Since immunoneutralization has been effective in inhibiting biological molecules, it was hypothesized that maternal immunization against myostatin in female mice might enhance muscle mass in offspring via myostatin-blockade in the developing embryos and neonates by maternally transferred anti-myostatin antibody. In this study, twenty reproducing, twelve week-old female mice were divided into four groups, and immunized against KLH (Control) or recombinant porcine mature myostatin (rMyo) or two different KLH-conjugated myostatin peptides (Myo-1 and Myo-2). Animals were immunized subcutaneously with 0.2 mg of immunogen mixed in TiterMax® adjuvant. Two or three boosters were administered prior to mating to ensure that the immunized female mice had significant antibody titers against their respective immunogens in ELISA. Sera collected from 3-day old neonates demonstrated significant titers, confirming the maternal transfer of anti-myostatin antibodies to offspring. However, no significant effects of immunization on the body weights of offspring were observed during 8 weeks of growout period. The offspring of the Myo-2 group had significantly heavier gastrocnemius and triceps muscles at 8 weeks compared to the controls ($P<0.01$), but the muscle mass of the offspring from the rMyo and Myo-1 groups did not

significantly differ from that of the control offspring. Since it is possible that the antibodies generated against three different antigens may have different binding characteristics and ability to inhibit myostatin activity, we examined the binding affinities of the antibodies to myostatin using Western blot analysis and the ability of the antibodies to suppress myostatin activity using pGL3 $(CAGA)_{12}$-Luc-luciferase reporter system. The antibodies from the three treatment groups showed affinity to mature myostatin monomer, but none of the antibodies showed affinity to myostatin dimer. In the pGL3 $(CAGA)_{12}$-Luc-luciferase reporter assay system, none of the antibodies from the three immunized groups showed the ability to suppress the biological activity of myostatin. In conclusion, we observed that the active immunization against myostatin using Myo-2 peptide improved the muscle growth of offspring. However, the inability of the anti-Myo-2 antibody to bind mature myostatin dimer and to suppress the myostatin's activity led us to question whether the improved muscle mass in the Myo-2 offspring was due to the inhibition of myostatin's biological activity by the anti-Myo-2 antibodies. Therefore, further studies are needed to determine whether active immunization against myostatin has the potential to improve skeletal muscle growth of offspring.

TABLE OF CONTENTS

LIST OF TABLES

LIST OF FIGURES

CHAPTER 1

LITERATURE REVIEW

1.1. Myostatin, a Negative Regulator of Skeletal Muscle Growth

Myostatin, also called as growth and differentiation factor-8 (GDF-8), is a potent negative regulator of skeletal muscle mass in many vertebrate species. Myostatin is a new member of the transforming growth factor–beta (TGF-β) superfamily of secreted growth factors (McPherron et al., 1997). Myostatin gene was first identified by screening murine DNA using PCR reaction with degenerated oligonucleotides corresponding to conserved sequences of the TGF-β superfamily members (McPherron et al., 1997). The same study also revealed the function of myostatin in murines, where targeted disruption of myostatin by gene knock-out resulted in 2-3 times greater muscle mass compared to the wild type mice (McPherron et al., 1997). The increased muscle mass in myostatin knock-out mice was found to be due to both muscle cell hyperplasia and hypertrophy.

Following the discovery of myostatin in 1997, natural mutations on myostatin gene were found be responsible for double-muscling in Belgian Blue and Piedmontese breeds of cattle (Grobet et al., 1997; Kambadur et al., 1997; McPherron and Lee, 1997). These cattle breeds have been selectively bred for ages because of their superior muscularity, although the molecular mechanisms underlying the double-muscling phenomenon was not known until recently. Similarly, a "*compact*" mutation in mouse, which was characterized by high protein content in the carcass, was also found to be due to a mutation on the myostatin gene (Szabo et al., 1998). Most recently, Schuelke et al. (2004) reported a natural mutation on myostatin gene in a hypermuscular human baby, suggesting the unique role of myostatin as a potent skeletal muscle inhibitor in humans

too, apart from other vertebrate species. In addition, studies indicate that myostatin gene and protein are well conserved across many vertebrate species (McPherron et al., 1997; Gonzalez-Cadavid et al., 1998; Ji et al., 1998; Ostbye et al., 2001; Roberts and Goetz, 2001). Taken together, these studies established myostatin as a unique negative regulator of skeletal muscle mass in many vertebrate species.

Myostatin is predominantly expressed in skeletal muscles as early as 9.5 days post-coitum and continues to be expressed throughout adulthood (McPherron et al., 1997). Myostatin expression has also been observed in other tissues apart from skeletal muscle in subsequent studies. Myostatin mRNA was noticed in both myogenic cells (myoblast) and non-myogenic cells (fibroblast) in regenerating skeletal muscle of the rat (Yamanouchi et al., 2000), in Perkinje fibers and cardiomyocytes in heart tissue (Sharma et al., 1999) and in tubuloalveolar secretory lobules of lactating mammary gland in pigs (Ji et al., 1998). In teleost fish, two distinct myostatin genes were identified (Ostbye et . al., 2001; Roberts and Goetz, 2001). Fish myostatin was detectable in numerous tissues including muscles, eyes, gill filaments, spleen, ovaries, gut, brain and testis (Rodgers et al., 2001; Maccatrozzo et al., 2001). The presence of myostatin in non-myogenic tissues suggests a possible role of myostatin in non-myogenic cell development and/or metabolism apart from regulation of skeletal muscle growth.

1.1.1. Myostatin gene

In cattle, the myostatin gene is located on chromosome2 (BTA2) at q11, where the double muscling (muscular hypertrophy; *mh*) locus had been mapped (Sonstegard et al., 1998[a]; Grobet et al., 1998). In human DNA, the myostatin gene was mapped to chromosome 2q (HSA2q) at q32·1, which is syntenic to the *mh* locus of double muscled

cattle (McPherron and Lee, 1997; Gonzalez-Cadavid et al., 1998). In pigs (Sonstegard et al., 1998[b]), mice (McPherron et al., 1997) and chickens (Sazanov et al., 1999), myostatin gene was mapped to chromosome 15 (15q2·3), chromosome 1 and chromosome 7 (GGA 7p11), respectively.

In human genome, the myostatin gene consists of three exons and two introns along with three transcription initiation sites, with no intron in the 5′-untranslated region upstream of the initiation codon (Gonzalez-Cadavid et al., 1998). Similarly, the porcine and bovine myostatin genes contain three exons and two introns (Stratil and Kopecny, 1999).

The human myostatin promoter region contains two upstream TATA boxes, an AP-1 transcription factor-binding site and a MyoD responsive element (Ferrell et al., 1999). It was also observed that human myostatin gene contained at least 5 SNP (single-nucleotide polymorphisms) sites in exons 1 and 2, but none in exon 3 (Ferrell et al., 1999). A recent analysis of 3.3-kb human myostatin promoter region depicted three TATA boxes, a partial CCAAT box, five octameric sequences homologous to the consensus binding sites of POU homeodomain proteins, twelve E boxes corresponding to MyoD binding sites, two regions homologous to MEF2 binding site, a putative peroxisome proliferators-activated receptor-γ (PPAR-γ) binding site and a region homologous to the consensus sequence of the nuclear factor (NF)-κB binding site (Ma et al., 2001). Furthermore, consensus sequences of various hormone-binding sites, including androgen response element, five sequences corresponding to three different glucocorticoid response elements [GRE, palindromic GRE (pal-GRE)], and tyrosine aminotransferase GRE (tat-GRE), three thyroid hormone response elements (TRE), three ER6 sequences that are known to have

similar function to TRE and two regions homologous to a cAMP responsive element were also identified (Ma et al., 2001).

The presence of responsive elements or binding sites to various biological molecules in the promoter region of myostatin gene indicates that myostatin gene expression is probably regulated by a complex interaction of various molecules that bind to the responsive elements. For instance, glucocorticoids found to have a stimulatory action on myostatin's expression since administration of dexamethasone, a glucocorticoid agonist, upregulated myostatin mRNA expression in rat skeletal muscles (Lang et al., 2001) and in muscle cell culture models (Ma et al., 2001). Conversely, dexamethasone-induced myostatin mRNA expression was inhibited by the administration of glucocorticoid antagonist, RU486 both *in vitro* and in rats (Ma et al., 2003). However, very little is known about the functional roles of other response elements on the regulation of myostatin expression, therefore more studies are needed to unravel the roles of various responsive elements in the myostatin promoter region.

1.1.2. Myostatin protein

Myostatin, being a member of TGF-β superfamily proteins, shares biochemical similarities with other members of the family. Myostatin is synthesized as a precursor protein composed a signal peptide, an N-terminal propeptide (prodomain) and a C-terminal mature/active domain (Zimmers et al., 2002). The signal peptide (24-amino acids) plays a role in the transport of myostatin precursor protein from the cytoplasm into endoplasmic reticulum, where it appears to be removed by the proteolytic processing prior to secretion outside the muscle cells. According to cDNA sequence analysis, the secreted precursor form of myostatin contains 375 AA in humans, baboons, cattle, pigs,

sheep, turkeys and chickens, while there are 376 AA in rodents (McPherron and Lee, 1997). The mature or active form of myostatin containing 109 AA is released upon removal of the N-terminal prodomain (latent peptide) by proteolysis at a conserved tetrabasic (RSRR) site mediated by a calcium-dependent serine protease called furin (Lee and McPherron, 2001; Thies et al., 2001). Recently, Jin et al. (2004) demonstrated porcine myostatin prepropetide as a substrate for furin proteases, confirming that the furin proteases mediate the cleavage of myostatin prepropeptide into prodomain and mature myostatin.

The AA composition in the mature form of myostatin is identical among human, mouse, rat, pig, chicken and turkey species and with only one AA difference in baboon, 2 AA difference in bovine and 3 AA difference in ovine species (McPherron and Lee, 1997). The mature form as well as the prepropeptide form of myostatin appears to form homodimers by disulfide-bonds similar to many other members of the TGF-β superfamily (McPherron et al., 1997; Lee and McPherron, 2001; Jin et al., 2004). However, the myostatin prodomain did not produce disulfide-linked homodimers (Lee and McPherron, 2001, Jin et al., 2004). The mature myostatin homodimer is widely regarded as the biologically active molecule that is capable of binding to *Act*RIIB receptors on skeletal muscle cells to exert its negative regulatory role on muscle mass (Lee and McPherron, 2001).

In Western blot analysis, two myostatin immunoreactive proteins were identified at 52 kD and 15 kD under reducing conditions in Chinese hamster ovary (CHO) cell culture homogenate that was transfected with murine myostatin expression construct, probably representing unprocessed precursor and mature form of myostatin, respectively

(McPherron et al., 1997). Under non-reducing conditions, two proteins at 101 kD and 25 kD were detected, indicating the homodimers of precursor and mature myostatin, respectively. The dimer formation of the mature myostatin was also demonstrated in several other studies (Wehling et al., 2000; Lee and McPherron, 2001; Thies et al., 2001; Jin et al., 2004). The apparent molecular weight of myostatin prodomain in SDS-PAGE was 37 kD (Lee and McPherron, 2001; Thies et al., 2001) weighing more than 27 kD, which is the predicted molecular weight of prodomain based on AA sequence. It was suggested that the discrepancy in estimated and apparent molecular weights was probably due to glycosylation of the myostatin prodomain (Lee and McPherron, 2001), which is a common characteristic of the TGF-β superfamily member proteins.

Many other studies also reported myostatin-immunoreactive proteins in skeletal muscle and serum using anti-myostatin antibodies. Four myostatin-immunoreactive proteins at 52 kD, 40 kD, 26 kD and at 30 kD were reported in bovine skeletal muscle (Sharma et al., 1999; Berry et al., 2002). Gonzalez-Cadavid et al. (1998) reported a 26 kD myostatin-immunoreactive protein under both reducing and non-reducing conditions in human skeletal muscles and in serum. The 26 kD band was explained as the mature myostatin protein that was glycosylated since it showed affinity to ConA-Sepharose column. Furthermore, a myostatin-immunoreactive protein at 30-32 kD was detected in rat skeletal muscles under both reducing and non-reducing conditions (Lalani et al., 2000; Sakuma et al., 2000; Kawada et al., 2001), and a 30 kD band was detected in the nuclear fraction in C_2C_{12} muscle cell culture (Artaza et al., 2002). Similarly, we noticed myostatin immunoreactive proteins at 50, 37, 30 and at 17 kD using a monoclonal antibody in chicken skeletal muscle but these bands were also identified in liver, small intestine and

brain apart from skeletal muscle (Kim et al., 2006). Hill et al. (2002) reported two myostatin-immunoreactive proteins (12 kD and 36 kD) separated by immuno-precipitation from mouse serum which were identified as mature myostatin and prodomain, respectively in LC-MS-MS. In another study, a 26 kD and a 12.5 kD bands were observed when a recombinant myostatin prepropetide was subjected to cleavage at the tetrabasic site, indicating the prodomain and mature myostatin, respectively (Zimmers et al., 2002). Furthermore, the 12.5 kD band was also observed in the serum from wild-type mice but not from myostatin-null mice under reducing conditions indicating mature myostatin (Zimmers et al., 2002). Based on the results from these two recent studies (Hill et al., 2002; Zimmers et al., 2002), it is suggested that some of the myostatin-immunoreactive proteins reported in other studies were probably non-myostatin proteins that had affinity to anti-myostatin antibodies in Western blot analyses.

1.1.3. Regulation of myostatin pre-receptor signaling

Many of the TGF- β superfamily growth factors exert their biological activities through their C-terminal mature/active protein dimer, which bind to specific receptors located on the cell membrane. Two types of transmembrane receptors, type II (*Act*RIIA and *Act*RIIB) and type I (ALK-4 and/or ALK-5), which exist in homodimers, located on the muscle cells were hypothesized to act as myostatin receptors (Lee and McPherron, 2001; Rebbapragada et al., 2003). In cross-linking studies, recombinant mature myostatin bound to activin type II receptors on COS-7 cells in a specific and saturable manner (Lee and McPherron, 2001). Furthermore, myostatin appeared to bind *Act*RIIB receptors with greater affinity than to *Act*RIIA receptors to initiate downstream signaling (Lee and McPherron, 2001; Rebbapragada et al., 2003) suggesting *Act*RIIB are crucial in

myostatin's signal transmission. Lee and McPherron, (2001) also generated transgenic mice overexpressing a dominant-negative form of *Act*RIIB that lacked kinase domain to examine the role of *Act*RIIB in mice. The transgenic mice demonstrated increased muscle mass with individual muscles weighing up to 125% compared to those of wild-type mice, suggesting the involvement of *Act*RIIB in myostatin signaling. Furthermore, administration of soluble forms of *Act*RIIB receptors in mice (Lee et al., 2005) appeared to have captured and prevented endogenous myostatin from binding to the *Act*RIIB receptors, leading to greater skeletal muscle mass that even exceeded the muscle mass of myostatin knockout mice. This finding not only confirms the role of *Act*RIIB in mediating myostatin signaling, but also suggests the existence of some unknown ligands, apart from myostatin, which may mediate through *Act*RIIB to inhibit muscle growth.

Previous studies suggested that the propeptides of TGF- β1, β2 and β3 associate non-covalently with their respective mature proteins to form latent complexes (Miyazono et al., 1988; Wakefield et al., 1988). Similarly, it was hypothesized that the regulation of myostatin's biological activity might also be controlled by the myostatin prodomain (McPherron et al., 1997; Thies et al., 2001; Lee and McPherron et al., 2001). In support, Lee and McPherron (2001) generated transgenic myostatin-prodomain overexpressing mice that showed 20-110% greater muscle mass compared to wild-type mice. In a similar study, transgenic mice overexpressing myostatin prodomain had shown increased muscle mass up to 40% than wild type mice (Yang et al., 2001). In agreement with the prodomain's role in regulating myostatin's biological activity, Thies et al. (2001) demonstrated that myostatin prodomain could inhibit binding of myostatin to L6 muscle cells.

In addition to prodomain, circulating myostatin has been found in association with follistatin (Lee and McPherron, 2001), follistatin related gene (FLRG) (Hill et al., 2002), titin-cap (Nicolas et al., 2002) and growth and differentiation factor-associated serum protein-1 (GASP-1) (Hill et al., 2003). Lee and McPherron (2001) demonstrated that the follistatin inhibits the binding of myostatin to *Act*RIIB in COS-7 muscle cell culture. The same study also demonstrated that transgenic overexpression of follistatin resulted in significant increases in muscle mass in mice, indicating an antagonistic role of follistatin on myostatin's activity (Lee and McPherron, 2001). In addition, follistatin could also inhibit myostatin's biological activity in pGL3 $(CAGA)_{12}$ luciferase reporter system with A204 muscle cell culture (Zimmers et al., 2002). Furthermore, follistatin has been shown to inhibit myostatin *in vivo* in chicken embryonic development where administration of follistatin resulted in greater skeletal muscle mass (Amthor et al., 2004). Similar to follistatin, FLRG, a highly similar protein, has also been shown to inhibit myostatin's activity in pGL3 $(CAGA)_{12}$ luciferase reporter system with COS1 cultures (Hill et al., 2002). Furthermore, titin-cap, a sarcomeric protein that binds to titin, appeared to prevent myostatin latent complex formation and inhibit myostatin secretion, since overexpression of titin-cap inhibited anti-proliferative activity of myostatin on C2C12 myoblasts without altering myostatin production or processing (Nicholas et al., 2002).

Recently, GASP-1, a novel member of the follistatin-domain protein family, has been found to interact with myostatin (Hill et al., 2003). In pGL3 $(CAGA)_{12}$ luciferase reporter assay system with A204 muscle cell culture, the GASP-1 was able to inhibit myostatin's activity, suggesting that GASP-1 acts as an inhibitor of myostatin's activity (Hill et al., 2003). Taken together, it appears that prodomain, follistatin, titin-cap and

GASP-1 interact with myostatin to regulate its biological activity most probably by inhibiting the binding of mature myostatin to *Act*RIIB receptors.

1.1.4. Post-receptor signaling of myostatin

Most of the TGF- ß family ligands bind to type II receptor homodimer first, and the ligand-type II receptor complex recruits a type I receptor homodimer leading to tetramerization of type I and II receptors (Reviewed by Massague, 1998; Derynck and Feng, 1997). It was hypothesized that myostatin activated *Act*RIIB transphosphorylates type I receptors (ALK-4 and/or ALK-5) in the intracytoplasmic domain to stimulate the serine/threonine kinase activity of type I receptors (reviewed by Massague, 1998). Rebbapragada et al. (2003) in cross-linking studies demonstrated that myostatin activated type II receptor associates with ALK-4 or ALK-5 (Type I receptors), indicating a similar post-receptor signaling event of myostatin in reference to other TGF- ß members.

Following type I and type II receptor tetramerization, signal is relayed downstream by a series of phosphorylations of intracellular Smad proteins that transduce the signal from the cell surface to the nucleus, where the downstream genes are up/down regulated. In mammals, eight different types of Smads have been identified and classified into three groups: the receptor-regulated Smads (R-Smads), common-partner Smads (Co-Smads) and inhibitory Smads (I-Smads) (Reviewed by Attisano and Wrana, 2000). Smad 2 and 3 appeared to transduce myostatin signal downstream since addition of myostatin upregulated both phospho-Smad-2 and phospho-Smad-3 in C2C12 myoblast cultures (Langley et al., 2002) and in C3H 10T1/2 cells (Rebbapragada et al., 2003). Interaction of phosphorylated Smad 2/3 with Co-Smad (Smad 4) has been found to be crucial, since co-transfection of Smad-4 construct was necessary to enable myostatin's signaling in

p(CAGA)12-MLP-Luc reporter assay with A204 cells (Zhu et al., 2004). Smads 2/3 along with Smad-4 form a heteromeric Smad-complex that in turn interacts with co-activators and co-repressors and eventually bind to DNA sequences to up/down-regulate the downstream genes (Reviewed by Massague and Gomis, 2006). In contrast, inhibitory Smads (Smurf-1 and Smad 7) prevent recruitment and activation of R-Smads forming a negative feedback loop to regulate myostatin-induced intracellular signaling (Reviewed by Zhu and Burgess, 2001). Zhu et al. (2004) demonstrated that either Smad-7 or Smurf-1 could partially reduce myostatin-induced luciferase signal by 50-60% and 40-50%, respectively, while co-transfection of both Smad-7 and Smurf-1 completely inhibited myostatin-induced luciferase signal, indicating both Smad-7 and Smurf-1 as inhibitory Smads for myostatin signaling. Furthermore, myostatin appears to auto-regulate its expression through Smad-7, since myostatin induced Smad-7 expression and the overexpression of Smad-7, in turn, inhibited myostatin promoter activity in C2C12 myoblast culture (Forbes et al., 2006). Although there is a very little definitive data to completely elucidate the myostatin downstream signaling, myostatin signaling appears to involve R-Smad 2 and 3, Co-Smad-4 along with two I-Smads, Smad-7 and Smurf-1 to establish a full Smad-regulatory loop in myostatin signaling. Figure 1.1 illustrates the putative elements in the myostatin signaling pathway (Adapted from Joulia and Cabello, 2006).

1.1.5. Physiological functions of myostatin

1.1.5.1. Role of myostatin in embryonic myoblast growth

The role of myostatin appears to be mostly confined to skeletal muscle growth, since the loss of myostatin activity resulted in a dramatic increase in skeletal muscle mass

without any significant effect on other organs (McPherron et al., 1997). C2C12 cell cultures when added with extraneous recombinant myostatin exhibited inhibition of myoblast proliferation (Thomas et al., 2000; Taylor et al., 2001; Langley et al., 2002). The inhibitory role of myostatin on myoblast proliferation was further supported by the coincidence of lower levels of myostatin mRNA expression with the myoblast proliferation period in chicken embryonic development and in satellite cell cultures (Kocamis et al., 1999 and 2001). In addition, hyperplasia of muscle fibers has been observed in mice and cattle carrying non-functional myostatin supporting the inhibitory role of myostatin on myoblast proliferation.

Myostatin appeared to inhibit proliferation of myoblasts by preventing the progression of myoblasts from G1-phase to S-phase of the cell cycle, which is regulated by Rb protein hypophosphorylation in C2C12 myoblast cultures (Thomas et al., 2000; Joulia et al., 2003). However, the proliferation was restored after removing myostatin from the cell culture indicating that the inhibitory effect of myostatin was reversible (Taylor et al., 2001). In addition, the myostatin-added muscle cell cultures showed the upregulation of p21, a cyclin-dependent kinase inhibitor, and downregulation of cyclin-dependent kinase-2 (Cdk2) with higher levels of hypophosphorylated pRb (retinoblastoma susceptibility gene product) (Thomas et al., 2000). Since Rb protein phosphorylation by Cdk physically releases E2F-DP1, a component that is needed for the transcription of S-phase-specific genes, by inhibiting the phosphorylation of Rb and its dissociation of E2F-DP1, myostatin ceases the cells in G0/G1 phase of cell cycle (Thomas et al., 2000; Joulia et al., 2003). Upregulation of p21 was also observed in C_2C_{12} muscle cell cultures over-expressing myostatin (Rios et al., 2001). These results suggest

that myostatin probably arrests the myoblast at G0/G1 phase of the cell cycle in a pRb-dependent pathway. In another study, myostatin inhibited myoblast proliferation by downregulating Cdk-2 and Cyclin E, without altering phosphorylation status of Rb in rhabdosarcoma cell cultures, indicating an Rb-independent pathway to inhibit myoblast proliferation (Langley et al., 2004). The inhibitory activity of myostatin on myoblast proliferation and differentiation was not only restricted to C2C12 myoblasts, since myostatin inhibited primary bovine fetal myoblast proliferation (Thomas et al., 2000), and implantation of myostatin-coated beads into developing chick limb buds down-regulated Myf5 and MyoD along with a decrease in the amount of limb muscle formed (Amthor et al., 2002).

Besides inhibiting myoblast proliferation, myostatin also appears to have a negative regulatory role in myoblast differentiation (Langley et al., 2002; Rios et al., 2002; Joulia et al., 2003). Myostatin inhibited myoblast differentiation in a dose-dependent manner in C2C12 myoblast culture, where downregulation of MyoD, Myf5, myogenin and p21 were observed (Langley et al., 2002). The downregulation of p21 was suggested to be due to myostatin's inhibition on p21 promoter activity during differentiation. Down-regulation of MyoD, myogenin and Myf5 was also observed in myostatin-treated myoblast cultures in two subsequent studies on C2C12 myoblast differentiation models (Rios et al., 2002; Joulia et al., 2003), indicating myostatin's role in inhibiting myoblast differentiation.

Addition of myostatin upregulated phosphorylated Smad-3 while inhibiting the proliferation of rhabdosarcoma cell cultures (Langley et al., 2002). On the other hand, lower levels of phosphorylated Smad 3/2 were observed upon the addition of anti-

myostatin antibody in cultured C_2C_{12} cells (Bogdanovich et al., 2002). These results suggest that myostatin requires Smad 2/3 activation in order to inhibit myoblast proliferation and differentiation by up-regulating p21 and down-regulating Cdk2, MyoD and other MRFs. The inhibitory activity of myostatin on myoblast proliferation and differentiation has been shown to be reversible by GH administration (Liu et al., 2003), suggesting a strong antagonism between GH and myostatin in skeletal muscle growth and metabolism. Figure 1.2 illustrates the role of myostatin on myoblast proliferation and differentiation.

1.1.5.2. Role of myostatin in postnatal skeletal muscle growth

The number of skeletal muscle fibers in many vertebrates appeared to be almost fixed once the embryonic proliferation phase has been completed (Goldspink, 1962; Rowe, 1969). However, certain degree of muscle cell proliferation has been observed after birth in some species since an increase in the number of muscle fibers during the neonatal period was noticed (Rayne and Crawford, 1975; Swatland, 1976; Wigmore and Stickland, 1983). The cross sectional area of muscle fiber in young animals is smaller and contains less number of nuclei than those of older animals. During the postnatal growth phase, mononucleated satellite cells, that are located between the basal lamina and sarcolemma of myofibers, proliferate, differentiate and fuse to existing muscle fibers, thus favoring postnatal muscle growth by providing additional myonuclei to adult muscle (Moss and Leblond, 1971; Schultz, 1996).

Numerous studies indicate that myostatin has a role in postnatal skeletal muscle growth and maintenance. Carlson et al. (1999) noticed upregulated myostatin mRNA in mouse gatrocnemius-plantaris muscles undergoing hind limb unloading prior to

significant muscle atrophy by third day after unloading. The mRNA levels were not significant after 3 to 7 days of hind limb unloading, suggesting that the myostatin upregulation probably induced the atrophy of skeletal muscles. In a similar study, Wheling et al. (2000) reported a 16 % decrease in plantaris mass and a 110 % increase in myostatin mRNA after 10 days of unloading. In agreement with the above results, 30-fold increase in the expression of myostatin mRNA was observed in both chronic and acute disuse-induced muscle atrophy (Reardon et al., 2001). Furthermore, Lalani et al. (2000) reported an increase in myostatin mRNA expression due to spaceflight-induced muscle atrophy, confirming the negative relationship between the myostatin mRNA expression and muscle mass.

Likewise, muscle regeneration models provided further insights confirming the negative relationship between myostatin and muscle regeneration. In rat skeletal muscles, myostatin mRNA was expressed in myogenic mononucleated cells during regeneration from necrosis induced by bupivacaine or hypertonic saline injection (Yamanouchi et al., 2000). In satellite cell culture derived from chicken muscles, temporal expression of myostatin mRNA started to increase when fusion of satellite cells to existing muscle fibers started, followed by a plateau for 144 hours showing the highest at 72 hours (Kocamis et al., 2001). In another study, myostatin mRNA levels declined gradually during degeneration caused by notexin injection, and the levels returned to the normal by the completion of regeneration at 28 days in rat soleus and extensor digitorum longus muscles (Mendler et al., 2000). These results suggest that myostatin expression is temporarily suppressed during the early stages of regeneration when satellite cell-derived

myoblasts proliferate, and the myostatin mRNA returns to normal levels after the completion of regeneration.

Additionally, studies suggest that the myostatin mRNA expression is dependent on the type of the muscle fibers. The expression of myostatin mRNA was detected to be higher in fast-type muscle compared to slow-type muscle (Mendler et al., 2000). In agreement with this finding, myostatin mRNA was found in great amounts in the white portion of mouse quadriceps muscle that was composed of 100 % type-IIB fast fibers (Carlson et al., 1999). Conversely, animal studies have shown that predominantly fast-type white muscle has low satellite cell densities compared to muscles that have predominantly slow-type red fibers, posing questions as to whether myostatin plays any role in postnatal muscle growth through satellite cell regulation (Carlson et al., 1999; Wehling et al., 2000).

The negative role of myostatin in postnatal skeletal muscle growth and maintenance was further elucidated by employing anti-myostatin antibodies to suppress the biological activity of myostatin. Bogdanovich et al. (2002) utilized *mdx* mice as an animal model for Duchenne muscular dystrophy to investigate the amelioration of muscular dystrophic condition by myostatin-blockade. They administered monoclonal anti-myostatin antibody that was generated against recombinant mature myostatin, and demonstrated a significant alleviation of dystrophic pathophysiology by 3 months of treatment with an increased whole muscle cross sectional area and muscle fiber area (Bogdanovich et al., 2002). Similarly, Whittemore et al. (2003) produced monoclonal anti-myostatin antibody by immunizing myostatin knockout mice with recombinant myostatin expressed in CHO cells. Administration of this antibody to mice resulted in

approximately 10 % increases in body weight and muscle mass compared to the controls, corroborating the efficacy of antibodies in blocking myostatin.

Yang et al., (2001) generated mice that overexpress myostatin prodomain in an effort to inhibit the biological activity of myostatin. These transgenic mice overexpressing prodomain, exhibited up to 40% greater skeletal muscle mass with significant hypertrophy of muscle fibers. In another study, male specific hypertrophy was achieved by generating transgenic mice expressing a dominant-negative myostatin propeptide under the control of myosin light chain 1F promoter and 1/3 enhancer from TSPY locus on the Y chromosome (Pirottin et al., 2005). The male transgenic mice demonstrated 5-20% increases in skeletal muscle mass, suggesting the gender-specific muscle mass enhancement, which could be useful in developing efficient cattle breeds where bulls could be optimized for beef production. On the other hand, Grobet et al. (2003) generated conditional myostatin knockout mice that demonstrated postnatal inactivation of myostatin, resulting in significant increases in muscle mass due to hypertrophy of muscle fibers comparable to myostatin knock-out mice generated by McPherron et al. (1997). Conversely, systemic over-expression of myostatin in mice resulted in dramatic reduction in muscle mass resembling the human cachectic condition (Zimmers at al., 2002), confirming the inhibitory role of myostatin on postnatal skeletal muscle growth. Recently, Magee et al., (2006) demonstrated reduced myostatin mRNA and protein expression by 27% and 48%, respectively by administering short hairpin interfering RNA (shRNA) against myostatin transcript in mice. They reported 10%, 34% and 100% increases in tibialis anterior weight, fiber size and satellite cell number, respectively, indicating that myostatin negatively regulates postnatal muscle mass, fiber

size and satellite cell number. In a recent study, young mice lacking myostatin demonstrated increased satellite cell number and activation level compared to wild type, and the difference was maintained as the mice aged (Siriett et al., 2006). Furthermore, muscle regeneration capacity was demonstrated to be better in myostatin-null muscle following notexin injury, indicating that prolonged absence of myostatin might rescue age-related sarcopenia by restoring muscle regenerative capacity (Siriett et al., 2006). In summary, these results suggest that myostatin has a negative role in postnatal muscle growth and maintenance by regulating the number of muscle fibers, size of muscle fibers and satellite cell activation.

1.1.5.3. Role of myostatin on adipose tissue metabolism

Myostatin-null mice had shown significantly low fat accumulation at any age compared to wild type mice without any significant changes in food intake and body temperature (McPherron and Lee, 2002). Conversely, transgenic mice overexpressing myostatin showed increased fat mass compared to wild type mice, which was observed only in males but not in females (Reisz-Porszasz et al., 2003), indicating the positive role of myostatin on adipogenesis. Lin et al. (2002) noticed significantly lower expression levels of peroxisome proliferator-activated receptor-γ (PPAR –γ) and CCAAT/enhancer binding protein –α (C/EBP-α), two transcription factors involved in adipogenesis, in myostatin knock-out mice compared to wild type. Therefore, it appears that the myostatin stimulates adipogenesis probably through the up-regulation of PPAR –γ and C/EBP-α. In support, Artaza et al. (2005) reported that the recombinant myostatin promotes the differentiation of multipotent mesenchymal cells (C3H10T1/2) into the adipogenic lineage while inhibiting myogenesis.

In another study, myostatin-propeptide overexpressing transgenic mice maintained normal blood glucose, insulin sensitivity and normal fat mass following a 2-month regimen with a high-fat diet (45% kcal from fat) compared to wild-type mice (Zhao et al., 2005). In a different study, the same transgenic mice, when challenged with a high-fat diet for 21 weeks, demonstrated 27% further muscle gain with no significant fat gain compared to normal-fat diet fed transgenics, while the wild-type mice gained 190% fat mass without no further muscle gain (Yang and Zhao, 2006). The same study also demonstrated larger adipocytes in the high-fat fed wild-type mice compared to high-fat fed transgenic mice, suggesting propeptide-mediated myostatin-blockade probably shifts the energy utilization toward skeletal muscle growth and maintenance from adipose tissue growth (Yang and Zhao, 2006).

In contrast to the above results, myostatin inhibited the differentiation of preadipocyte into adipocyte *in vitro* (Kim et al., 2001). In this study, the addition of recombinant myostatin to 3T3-L1 adipose cell culture reduced the expression levels of PPAR–γ and C/EBP-α, along with the reduced morphological pattern of differentiation, suggesting the myostatin's inhibitory role on adipocyte differentiation. In agreement, myostatin inhibited the differentiation of bovine preadipocytes through downregulating the expression levels of PPAR–γ and C/EBP-α, even at a lower dose than that inhibited myoblast differentiation (Hirai et al., 2007).

Interestingly, myostatin appeared to trigger the formation of immature adipocytes but with favorable metabolic effects in C3H10T1/2 pluripotent cell cultures and also in myostatin-overexpressing transgenic mice (Feldman et al., 2006). This study also demonstrated significant increases in insulin sensitivity and resistance to obesity in

myostatin-overexpressing transgenic mice confirming the favorable metabolic effects of myostatin. However, myostatin failed to induce adipogenesis in 3T3-L1 preadipocyte culture, which were more differentiated in adipocyte lineage than C3H10T1/2 pluripotent cell cultures. Therefore, myostatin appears to trigger adipogenesis at a pluripotent cell stage than at an already differentiated stage, indicating a sensitive period of proadipogenic activity of myostatin on early-undifferentiated cells and antiadipogenic activity on already differentiated preadipocytes. This hypothesis probably explains the seemingly constrasting previous findings of myostatin action on adipogenesis. Taken together, myostatin appears to promote adipogenesis, and conversely, absence of myostatin / myostatin-blockade minimizes the adiposity with favorable metabolic effects. Nevertheless, in the wake of conflicting results, further studies are needed to elucidate the exact role of myostatin on adipogenesis.

1.2. Enhancing Animal Growth Potential through Manipulating Growth Regulators

1.2.1. Immuno-neutralization of biological molecules

Antibodies have been extensively utilized in modulating the biological activities of target molecules via passive immunization or active immunization protocols. The classical view of antibody function is that the antibody binds to the target molecule and form immune complex, which is subsequently removed by reticulo-endothelial system leading to the activity-blockade of target molecule (Reviewed by Pell, 1997). Active immunization, which is generating endogenous antibodies in the host by injecting small amounts of foreign antigen, has been found to be more effective with fewer side effects

than passive immunization or administration of exogenous antibodies developed in another animal (Reviewed by Zagury and Gallo, 2004).

Passive immunization by administering antibodies against ACTH (Adreno Cortico-Tropic Hormone), a stress-induced corticosteroid that retards growth rate, has been shown to inhibit ACTH, which was evidenced by 59 % reduction in peak plasma corticosteroid level and 37% increase in the body weight in rats (Sillence et al., 1992). Similarly, myostatin-blockade by monoclonal antibodies resulted in significant increases in muscle mass in rodents (Bogdanovich et al., 2002; Whittemore et al., 2003), indicating the inhibitory role of antibodies on myostatin's activity. Recently, we demonstrated enhancement of post-hatch broiler muscle growth by *in ovo* administration of monoclonal anti-myostatin antibody (Kim et al., 2006). Nevertheless, long-term passive immunizations speculated to have half-life less than 3 wks and may have adverse effects by eliciting anti-idiotype antibodies leading to undesirable physiological consequences (Reviewed by Zagury and Gallo, 2004; Pell and Aston, 1995).

Alternatively, active immunization against biological molecules appears to be more practically feasible in maintaining antibodies against targeted molecules on a long-term basis. Active immunization against somatostatin, a hormone that inhibits the biological activity of growth hormone, improved growth rates in sheep (Spencer et al., 1983). In another study, active immunization against cholecystokinin (CCK), a gastric enzyme responsible for satiety, increased the feed intake and body weights by 5.4% and 8.35 %, respectively (Pekas and Trout, 1990). Similarly, active immunization against gonadotropic releasing factor (GnRF) with GnRF-KLH conjugate in 4 months-old bull calves resulted in significant reduction in testicular growth and masculinity (Adams et al.,

1993). In a similar study, administration of GnRH conjugated to human serum albumin (HSA) in heifers resulted in anestrous with reduced plasma estradiol, arrested follicular growth and reduced ovulations, indicating the efficiency of active immunization against GnRH in heifers (Prendiville et al., 1995). Huxsoll et al. (1998) reported that active immunization with anti-GnRH vaccine in bulls and steers reduced aggressive behavior and improved carcass quality. Most recently, active immunization against male sex hormone (GnRF) has been commercialized as an alternative to surgical castration (Improvac™) to remove boar taint in pigs (Dunshea et al., 2001). Furthermore, in gilts, administration of anti-GnRF vaccine resulted in reduced ovary size and maturity, indicating that the anti-GnRF effect is equally effective in gilts (McCauley et al., 2003). These studies indicate that active immunization may be an effective strategy in modulating the biological activities of target molecules for agricultural purposes.

However, passive administration of antibodies against growth hormone (Holder et al., 1985), thyrotropin (Holder et al., 1987), cholecystokinin (Spencer 1992) and IGF-1 (Stewart et al., 1993) did not appear to inhibit the respective target molecules, instead the antibodies appeared to have potentiated the biological activities of the respective target molecules. Although the principles underlying the potentiation effect are not completely understood to date, it was hypothesized that the antibodies may enhance the activity of target molecule by extending its half-life, by protecting the target molecule from degradation or by assisting in its transport and delivery to the target tissues (Reviewed by Pell, 1997).

Active immunization against foreign proteins or peptides has been extensively studied as with the development of vaccines against various diseases. However, induction

of antibodies against self-antigens demonstrated variable responsiveness, characterized by their ability to inhibit, mimic or potentiate the biological activities of target molecules (Reviewed by Pell, 2007). The underlying mechanisms of this variable responsiveness are not yet completely elucidated. Self-antigens that are conjugated to KLH (Key-hole limpet hemocyanin), a foreign T-helper carrier protein, found to be capable of eliciting antibodies toward self-antigens, probably by evading the innate clonal ignorance, clonal deletion and clonal anergy, which usually prevent the production of antibodies toward self-antigens (Reviewed by Zagury et al., 2003). Although the underlying principles of active immunization against self-proteins were not adequately elucidated, this strategy appears to be effective in attaining desirable physiological responses in both human health and animal production sectors.

1.2.2. Maternal transfer of antibodies to offspring in mice

Maternal adaptive immunity has a strong influence on the immune responses of the offspring. Many mammalian species show maternal transfer of antibodies to offspring in order to protect the newborn offspring from various diseases, and they might actively shape childhood immunity and tolerance induction by providing the fetus or infant with mother's immunological experience (reviewed by Zinkernagel, 2001). Maternal immunoglobulins are transferred to fetus or neonate through placental and lactational transmission. Among the five classes of immunoglobulins, IgG has shown placental transfer to the neonates in rodents (Roberts et al., 1990; Ahouse et al., 1993). During the first trimester of pregnancy, very little IgG is transported to the fetus in mice (Gitlin and Morphis, 1969). However, toward the term, fetal IgG concentrations match up with maternal IgG levels in humans and pigs (Longsworth et al., 1945; Kohler et al., 1966).

During gestation, IgG isotypes cross the placenta and enters the blood stream of the fetus with the help of FcRn receptor, a special transporter protein that mediates the transport of IgG across the syncytiotrophoblast layer, which is a barrier tissue between maternal and fetal circulation in placenta. FcRn was later found be related to MHC class I proteins and was detected in rat and mouse yolk sacs (Roberts et al., 1990; Ahouse et al., 1993). Although, the exact transport of IgG across the vascular endothelium is not completely understood, the FcRn appears to carry IgG into fetal circulation avoiding intracellular degradation of the IgG in rodents and humans (Simister et al., 1996 and 2003).

Mouse colostrum or breast milk contains high levels of IgG compared to IgA and IgM (Reviewed by Van-De Perre, 2003). The suckling neonates absorb IgG, IgM and IgA through FcRn receptors located on duodenal and jejunal enterocyte membranes (Simpson-Morgan et al., 1972; Simister et al., 1985; Israel et al., 1995). Furthermore, Milk IgG has been shown to be transferred from the intestinal lumen to circulation in neonatal mice (Simpson-Morgan et al., 1972). Although these studies documented the placental and lactational maternal antibody transfer to offspring, very little is known about the exact mechanisms involved in both of these phenomena.

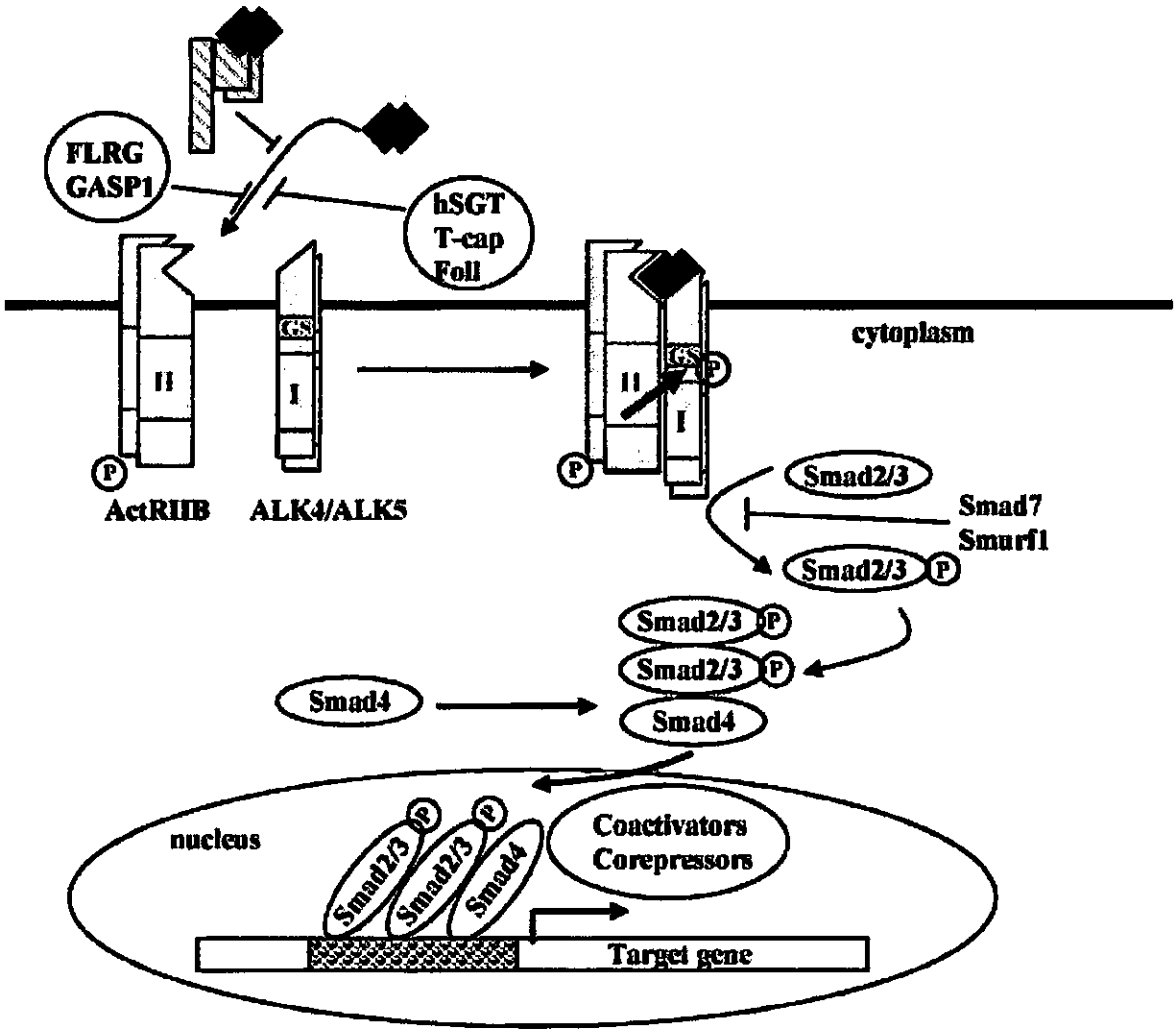

(Adapted from Joulia and Cabello, 2006)

Figure 1.1. Molecular factors involved in myostatin signaling. Myostatin is kept inactive when bound to FLRG, GASP-1, hSGT, T-cap, follistatin or to the myostatin propeptide. The active myostatin dimer binds to the *Act*RIIB receptor, which in turn interacts with the *Act*RI receptor (ALK4 or ALK5) by transphosphorylation. The tetrameric receptor complex recruits smads, the intracellular signal transducers. Smad2 and Smad3 aggregate with Smad4 and are translocated to the nucleus, activating target gene transcription. The inhibitory smads (Smad7 and Smurf1) constitutes negative loop to negate Smad2/3 signaling. Smad7 represses the myostatin signal by binding its MH2 domain to activated receptors, thus preventing recruitment and activation Smad 2/3. Smurf1 is an E3 ubiquitin ligase that mediates ubiquitination and consecutive degradation of Smad 2/3.

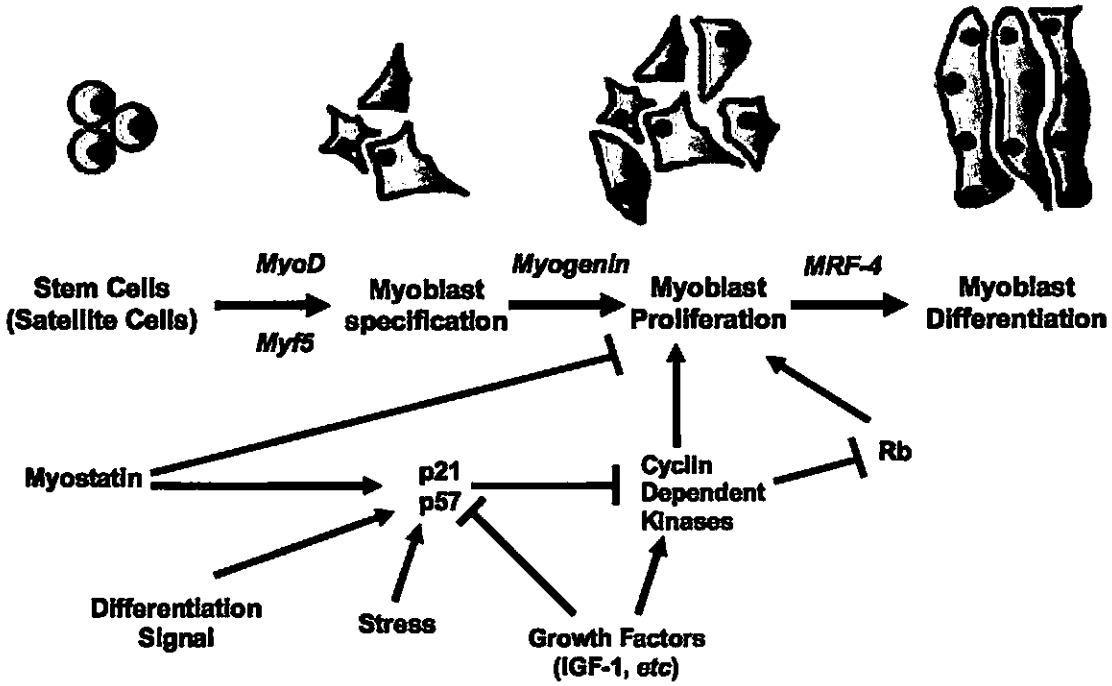

(Source: Lee SJ, 2004)

Figure 1.2. Myostatin and Myogenesis. Role of myostatin as a negative regulator of myogenesis in relation to other molecular cues that promote myoblast proliferation and differentiation. Myogenic Regulatory Factors (MyoD, Myf5, Myogenin and MRF-4) are required for the normal myoblast proliferation and differentiation.

CHAPTER 2

EFFECTS OF MATERNAL IMMUNIZATION AGAINST MYOSTATIN ON POST-NATAL SKELETAL MUSCLE MASS OF OFFSPRING IN MICE

2.1. INTRODUCTION

Myostatin, a member of the TGF-β superfamily of growth factors, is a potent negative regulator of skeletal muscle growth. Myostatin gene knockout demonstrated 2-3 times greater skeletal muscle mass in mice through muscle cell hyperplasia and hypertrophy (McPherron et al., 1997). A natural mutation on myostatin gene resulted in double-muscled cattle breeds like Belgian Blue and Piedmontese (McPherron and Lee, 1997; Grobet et al., 1997; Kambadur et al., 1997). Recently, Schuelke et al. (2004) reported a natural mutation on the myostatin gene in a hypermuscular human baby implicating the role of myostatin as a unique muscle growth inhibitor in humans too, as in many other vertebrate species.

Mature myostatin protein, like many other TGF- β members, forms a homodimer that is capable of binding to *Act*RIIB receptors located on the muscle cells to exert its negative regulatory role on skeletal muscle growth (Lee et al., 2001). Myostatin-binding proteins including myostatin propeptide, follistatin, follistatin related gene (FLRG) and growth and differentiation factor-associated serum protein-1 (GASP-1) render mature myostatin latent and inactive (McPherron et al., 2001; Hill et al., 2002; Wolfman et al., 2003). Prevention of binding of mature myostatin dimer to *Act*RIIB receptors by anti-myostatin antibodies (Bogdanovich et al., 2002; Whittemore et al., 2003), overexpression of prodomain (Lee et al., 2001; Yang et al., 2001), overexpression of follistatin (Lee et al., 2001) and by administration of soluble forms of *Act*RIIB receptors (Lee et al., 2005)

resulted in greater skeletal muscle mass with less fat accretion in mice. These studies indicate the potential of myostatin-blockade to enhance muscle growth for agricultural and human therapeutic applications. Among various ways to block or neutralize myostatin, it appears that immunoneutralization is an effective method applicable to animal production industry. In support, we recently demonstrated that *in-ovo* administration of monoclonal anti-myostatin antibody enhances post-hatch muscle mass in broilers (Kim et al., 2006).

Alternatively, active immunization against myostatin has been postulated to be practically feasible for agricultural applications. Recently, active immunization against male sex hormone (GnRF, gonadotropin-releasing factor) has been commercialized as an alternative (Improvac™) to surgical castration to remove boar taint in pigs (Dunshea et al., 2001). Active immunization, apart from eliciting antibodies, also confers placental transfer of antibodies to offspring (mostly IgG subclass) and secretion of antibodies in milk (IgG, IgM and IgA) in mice (Roberts et al., 1990; Ahouse et al., 1993). Therefore, we hypothesized that maternal transfer of anti-myostatin antibodies from the immunized female mice to their developing embryos and neonates may inhibit endogenous myostatin in the offspring, leading to greater muscle mass in offspring. Since maternal transfer of immunoglobulins is well established and several antibody-mediated myostatin-blockade experiments were successfully demonstrated in mice, in this study, we investigated the effects of maternal immunization against myostatin on the post-natal skeletal muscle mass of offspring in mice.

2.2. MATERIALS AND METHODS

2.1.1. Myostatin immunogens

Three different myostatin antigens consisting of different AA sequences were prepared: rMyo, an *E.coli* derived recombinant mature myostatin protein (Kim et al., 2006) and two small peptides (Myo-1 and Myo-2) located on the mature myostatin. The AA sequence of rMyo was LEVRVTDTPKRSRRDFGLDCDEHSTESRCCRYPLTV DFEAFGWDWIIAPKRYKANYCSGECEFVFLQKYPHTHLVHQANPRGSAGPC CTPTKMSPINMLYFNG KEQIIYGKIPAMVVDRCGCS representing the 103 AA-length mature myostatin. The AA sequences of Myo-1 and Myo-2 fragments were MSP INM LYF NGK EQI IYG KIP AMV and V FLQ KYP HTH LVH QA, representing AA sequences from 79 to 102 (Myo-1) and from 50 to 64 (Myo-2) on the mature myostatin, respectively (Figure 2.1). Myo-1 and Myo-2 peptides were commercially synthesized and conjugated to keyhole limpet hemocyanin (KLH). A cysteine-glycine sequence was inserted at the N-terminal side of the peptides during synthesis to allow a thio-ether linkage during the conjugation to carrier proteins. LC-SMCC, a sulfhydryl- and amine-reactive heterobifunctional crosslinking agent (Pierce, Rockford, IL), was used for conjugation of peptides to the carrier protein. Figure 2.2 (3-D model) illustrates the structure of myostatin monomer, two of which constistutes rMyo as a dimer, and the location of Myo-1 and Myo-2 peptides on myostatin monomer. The Immunogens were prepared in 1:1, PBS and Titermax® adjuvant emulsion (Titermax Inc. Norcross, GA).

2.2.2. Immunization of female mice against myostatin and sera collection

Twenty 12 wk old female B6SJLF-6 Taconic strain mice, obtained through LAS facility, UH Manoa, were randomly assigned into four groups: Control, rMyo, Myo-1 and

Myo-2, with 5 mice in each group. Female mice were injected with 0.2 mg immunogen in 100 µl of 1:1 PBS and Titermax® adjuvant (Titermax USA Inc, Norcross, GA) emulsion subcutaneously below the base of tail or around the neck. Controls received 1:1 PBS and Titermax® adjuvant. Booster doses were administered at the same dose (0.2 mg/mouse) 2-3 weeks apart after primary immunization for 2-3 times based on the titer levels, and mice were allowed to breed once they showed significant sera titers. Blood was collected by tail scission at 2 wks after primary immunization or booster, stored at 4°C overnight, and centrifuged at 3000 rpm for serum collection. The sera collected were screened for antibody titers using ELISA with three different coating antigens. After whelping, one 3-day old pup from each litter was sacrificed for serum collection to evaluate maternal transfer of antibody to offspring using ELISA.

2.2.3. Housing and breeding

The mice were housed in the laboratory animal facility at 12hr/12hr light-dark cycles. All of the procedures of animal care and handling were approved by IACUC, University of Hawaii at Manoa. Mice were fed with a commercial diet and clean water *ad libitum*. The immunized female mice with significant sera titers were allowed to breed with four males randomly with 3-day rotations until the mice exhibited the external signs of pregnancy. Pregnant mice were housed individually and non-pregnant mice received one more booster and set to breed until they became pregnant. After whelping, total weight of littermates from each mouse was recorded until the pups were weaned at 3 weeks of age. After weaning, male and female littermates from each immunized female mouse were recorded separately until 8 weeks of age. The offspring were sacrificed at 8 weeks of age and carcass characteristics: carcass wt, gastrocnemius, triceps,

parametrial/epididymal fat, were recorded. The immunized female mice, after weaning, received one more booster and were sacrificed after 2 weeks for serum collection.

2.2.4. Enzyme-linked immunosorbent assay (ELISA)

Three coating antigens were used for ELISA: rupMyo, a recombinant unprocessed porcine mature myostatin protein expressed in *E.coli* (Jin et al., 2004), Myo-1-BSA conjugate and Myo-2-BSA conjugate. A 96-well micro-ELISA plate was coated with 50 µl of coating antigen (10 µg/ml) per well and incubated overnight at 4°C. The plate was washed once with phosphate buffered saline (PBS: 20 mM sodium phosphate, 15 mM NaCl, pH 7.4), blocked with 100 µl of 1% BSA in PBS per well, and incubated for two hours at room temperature. The plate was washed twice with PBS-0.05 % Tween-20, and 50 µl of antisera in various dilutions were added, followed by incubation for 1 hour at room temperature. After incubation, the plate was washed thrice with PBS-0.05 % Tween-20, and 50 µl of anti-mouse IgG alkaline phosphatase conjugate (secondary antibody) in PBS-0.05 % Tween-20 at 1:20,000 dilution was added, followed by incubation for 1 hour at room temperature. The plate was washed thrice with PBS-0.05 % Tween-20, and 50 µl of 4- nitrophenyl phosphate (pNPP) was added per well, followed by incubation for 20-30 minutes in the dark at room temperature. The reaction was halted by the addition of 25 µl of 3 N NaOH, and the OD was measured at 405 nm using a microplate reader. Assay was performed in duplicate with a non-antigen coated reference control well, which serves as non-specific binding control. The average OD of the duplicate wells was corrected to the reference control well to derive the absolute OD units, which were expressed as antibody titers.

2.2.5. Affinity-purification of anti-myostatin antibodies from immune sera

Antibodies were purified from immune sera using Protein-A affinity chromatography with a commercially available buffer system (Affi-gel protein A MAPS® II kit from Bio-Rad, Hercules, CA). Combined serum from the five immunized female mice in each group was diluted with equal volume of binding buffer (MAPS II binding buffer), centrifuged at 12,000 g and filtered through a sterile 0.22 μ filter (Millipore®, Billerica, MA). The diluted serum was loaded onto a Protein-A affinity column previously equilibrated with 5 bed volumes of binding buffer, followed by washing with 15 volumes of binding buffer. IgG was eluted with 5 bed volumes of the elution buffer (MAPS II elution buffer), and 0.5 ml fractions were collected in tubes containing 100 μl of 1 M Tris buffer (pH 8.0). The fractions were desalted using dialysis against PBS overnight. The purified IgGs were analyzed by SDS-PAGE under both reducing and non-reducing conditions to determine the purity of antibodies.

2.2.6. Protein assay

Sample protein concentrations were determined by either the Lowry method (1951) or the Bradford method (1976) using bovine serum albumin (BSA) as a standard protein at 280 nm using a spectrophotometer.

2.2.7. Sodium dodecyl sulphate - polyacrylamide gel electrophoresis (SDS-PAGE)

SDS-PAGE was performed on mini gels (9 x10 cm) by the method of Laemmli (1970) using 15% polyacrylamide gels in the presence of 0.1% SDS under reducing (with 2-mercaptoethanol) or non-reducing conditions. Mouse skeletal muscle and liver tissues were homogenized in 10 volumes of sodium phosphate buffer (10 mM sodium phosphate monobasic and 10 mM sodium phosphate dibasic with 0.1% SDS, pH 7.0) on ice. The

homogenates were centrifuged at 12,000 g for 10 minutes to remove insoluble material and were used as reference tissue controls. Mature form of myostatin (R&D systems, Minneapolis, MN) in reducing or non-reducing condition, skeletal muscle and liver homogenates were subjected to 15% SDS-PAGE. The gels were stained with Coomassie blue to visualize the protein bands or the proteins were transferred onto a PVDF membrane for Western blot analysis.

2.2.8. Western blot analysis

Antibody binding affinity to myostatin was determined using Western transfer and immunoblotting. Proteins were electrophoretically transferred onto PVDF membrane while immersed in Towbin buffer (25 mM Tris, 192 mM glycine, 20% methanol, 0.1% SDS). After transfer, membranes were blocked with BM® blocking solution (Boehringer Mannheim, Indianapolis, IN) at 4°C overnight. Membranes were then incubated with 2 μg/ml of affinity purified IgG in TBS buffer (125 mM NaCl, 25 mM Tris, pH 8.0) for 1 hour at room temperature. After three, 10-minute washings with TTBS buffer (125 mM NaCl, 25 mM Tris, pH 8.0 containing 0.5% Tween-20), membranes were incubated with 1:10,000 alkaline phosphatase conjugated anti-mouse IgG (Sigma, St. Louis, MO) in TBS for 1 hour at room temperature. After three, 10-minute washings with TTBS buffer, membranes were developed using BCIP/NBT substrate (Nitroblue tetrazolium and Bromo-chloro-indolyl phosphate from Pierce, Rockford, IL). Membranes were air dried in a cool dark place for 1-2 hours at room temperature and the images were captured by Bio-Rad multi-imager, Bio-Rad, Hercules, CA.

2.2.9. pGL3 $(CAGA)_{12}$ Luc-luciferase reporter system

The pGL3 $(CAGA)_{12}$ Luc-luciferase reporter plasmid construct contains twelve CAGA sequences in the promoter region which are responsive to Smad proteins induced by TGF-ß family members, including myostatin. The plasmid construct contains firefly luciferase gene next to the promoter, which is designed to induce luciferase production upon myostatin activity. The pGL3 $(CAGA)_{12}$ Luc-luciferase plasmid was constructed as described by Dennler et al., (1998) and was a gift from Dr. Kunihiro Tsuchida from the University of Tokushima, Japan. In order to normalize the transfection variation among different wells, the pGL3 $(CAGA)_{12}$ Luc-luciferase plasmid was co-transfected with pRL-TK-Renilla luciferase plasmid construct (Promega, Madison, WI), which has a constant expression level.

A204 cell line of human rhabdosarcoma cells were seeded at 40,000 cells/well in a 96-well microculture plate and were grown in DMEM containing 10% fetal calf serum (FCS), antibiotic and antimycotic at 37.5° C and 5% CO_2. After 36 hours, medium was removed and cells were transfected with a mixture of pGL3 $(CAGA)_{12}$ Luc-luciferase plasmid (0.4 µg/well), pRL-TK-Renilla luciferase plasmid (0.05 µg/well) and lipofectamine (0.2 µl/well) in DMEM with 10% FCS but without antibiotic/antimycotic. After 24 hrs, cells were serum starved for 9 hrs. Following serum starvation, 5 ng/ml myostatin dimer, along with serial dilutions of affinity-purified IgG or 30 ng/ml of myostatin prodomain were added. After 6-8 hrs of incubation, luciferase activity was measured by Dual Luciferase Assay System (Promega, Madison, WI) using Veritas® luminometer (Turner Biosystems Inc, Sunnyvale, CA). The data were represented as the ratios of firefly luciferase to renilla luciferase activity in bar diagrams.

2.2.10. Statistical analysis

The body weights and carcass characteristics were analyzed by GLM procedure using JMP® software (SAS Institute, Cary, NC). Model included main effects of treatment and sex and treatment-sex interaction. Firefly luciferase/renilla luciferase ratios were analyzed by one-way ANOVA. Means differences were analyzed by Tukeys-HSD test or students-t test when a significant difference was observed.

2.3. RESULTS

2.3.1. Serum antibody titer dynamics in immunized female mice

Sera titers were evaluated by ELISA using three different coating antigens: rupMyo, a recombinant unprocessed porcine myostatin protein that demonstrated binding affinity to anti-myostatin antibody (Jin et al., 2004), Myo-1-BSA conjugate and Myo-2-BSA conjugate. Table 2.1 shows the sera titer dynamics following the primary immunization and subsequent boosters. All treatment groups developed increasing titers after primary immunization and boosters, indicating the escalating antibody levels. Control group that received adjuvant only, did not show titers against any of the coating antigens. The titer dynamics also indicate that the rMyo and Myo-1 elicited a quicker immune response than Myo-2. Table 2.2 shows the average sera titers of immunized female mice just before breeding at 1:250 dilution. With rupMyo coating antigen, Myo-1 sera showed greater affinity (0.526), while rMyo (0.228) and Myo-2 (0.302) sera affinities were lower. Against Myo-1 coating antigen, Myo-1 and rMyo sera titers were 0.410 and 0.165 respectively, while Myo-2 sera did not cross-react with Myo-1 coating antigen. Against Myo-2 coating antigen, Myo-2 sera showed 0.573, while rMyo and Myo-1 sera did not show significant titers. The crossreactivity of particular serum to another similar coating antigen, besides its respective coating antigen, reflects the antigenic similarities among rMyo, Myo-1 and Myo-2 immunogens. As expected, Myo-1 and Myo-2 immunogens appeared unique and did not elicit antibodies that crossreact with Myo-2 and Myo-1 coating antigens, respectively.

2.3.2. Effect of active immunization on body weights of immunized female mice

Table 2.3 shows the weekly body weights of immunized female mice during the immunization regimen. During this period, no significant differences in body weights were observed among the immunized groups, indicating that active immunization against myostatin did not modulate the body weights of the immunized female mice. Two mice in rMyo group, one each in Myo1 and Myo-2 groups did not conceive due to unknown reasons.

2.3.3. Maternal transfer of anti-myostatin antibodies to the offspring

Table 2.4 shows the average sera titers of the 3-day old neonates at 1:250 dilution. As expected, sera from the control group pups did not react with any of the coating antigen, and the sera affinity profiles of other treatment group litters were similar to those of their respective immunized mothers. Myo-1 group pups had shown high affinity (0.245) to rupMyo coating antigen, while the titers of rMyo (0.076) and Myo-2 (0.053) pups were significantly lower. Myo-1 group pups had an average titer around 0.050 against Myo-1 coating antigen, while rMyo and Myo-2 pups showed none. Myo-2 group pups showed significantly higher titer (0.178) toward Myo-2 coating antigen, while rMyo and Myo-1 group pups did not show significant affinity. Although the titers appeared relatively low in 3-day old neonates compared to their dams, these results confirmed the presence of maternally transferred anti-myostatin antibody in the offspring. Furthermore, the antibody binding affinities of neonatal sera were similar to those of their immunized dams. However, we noticed a significant variability in titers within each treatment group litters, probably indicating variable levels of antibody transfer to the litters.

2.3.4. Effect of maternal immunization on the body weights of offspring

Entire litter from each immunized female mouse was weighed collectively until they were weaned on third week, and total male or female littermates from each dam were separately weighed thereafter. Table 2.5 shows the average body weights of littermates until they were sacrificed at 8^{th} wk. Despite evident maternal transfer of antibody to the offspring, no significant differences in the body weights were observed among the litters until 7 wks post-partum. However, the Myo-2 group offspring tended to weigh slightly heavier at 8^{th} wk than the control offspring ($P= 0.056$), regardless of sex.

2.3.5. Effect of maternal immunization on the carcass composition of offspring

Table 2.6 shows the carcass characteristics of the offspring at 8 wks of age. Male offspring, had heavier body wt, carcass wt, carcass %, gastrocnemius, gastrocnemius % to the body wt, triceps, triceps, triceps % to body wt, visceral fat and visceral fat % to the body wt ($P<0.001$), compared to female offspring. We observed that the gastrocnemius and triceps were significantly heavier in only Myo-2 offspring by 8.75 % and 11.96 %, respectively ($p<0.001$), compared to controls, regardless of sex. There was a significant interaction of visceral fat mass with sex, which signifies that the males accrued lesser fat mass and females accrued greater fat mass in both rMyo and Myo-1 offsprings, compared to the control offspring (Table 2.7). However, the visceral fat mass in Myo-2 offspring was significantly greater than control offspring, regardless of sex.

2.3.6. Western blot binding characteristics of immune sera

The sera from all female mice in each immunized group were pooled and IgGs were purified using protein A affinity chromatography. The binding affinity of purified IgGs to the murine mature myostatin monomer and dimer was characterized in Western

blot analysis (Fig. 2.3). Purified IgG from the three treatment groups showed affinity to mature myostatin monomer (14 kD) but none of the IgGs showed affinity to mature myostatin dimer (26 kD). Based on the band intensity, the binding affinity of Myo-1 IgG appeared to be greatest, followed by rMyo and Myo-2 IgGs. Faint bands in the skeletal muscle tissue lane did not match with the known molecular wts of myostatin proteins, indicating that the binding was probably non-specific.

2.3.7. Effects of purified antibodies on pGL3 (CAGA)$_{12}$ Luc-luciferase reporter system

Affinity-purified IgGs were evaluated for their ability to inhibit myostatin's biological activity on A 204 skeletal muscle cells. The pGL3 (CAGA)$_{12}$ Luc-luciferase plasmid reporter system has been widely used to evaluate the activities of several members of TGF-ß family, including myostatin. Normally, a 5 ng/ml of recombinant mature myostatin dimer (R&D systems, Minneapolis, MN) could initiate firefly luciferase activity to an optimal extent. Myostatin prodomain, being an inhibitor of myostatin activity, at as low as 30 ng/ml could block the firefly luciferase signal almost completely ($P < 0.001$) by binding to mature myostatin dimer and forming a latent complex. However, the purified IgGs from the sera of the immunized mice did not have significant effect on the firefly luciferase activity, indicating that the antibodies perhaps were unable to inhibit the biological activity of myostatin (Fig. 2.4).

2.4. DISCUSSION

Disruption of myostatin activity via passive administration of anti-myostatin antibodies has resulted in greater muscle mass in mice (Bogdanovich et al., 2002; Whittemore et al., 2003). Similarly, we have shown that *in ovo* administration of monoclonal anti-myostatin antibodies enhances post-hatch broiler muscle mass (Kim et al., 2006). These studies illustrate the potential of immunoneutralization of myostatin in enhancing muscle mass in farm animals. Since active immunization confers maternal transfer of antibody to the offspring through placenta and colostrum, we hypothesized that maternal immunization against myostatin may enhance the skeletal muscle mass in offspring.

In this study, we used three different myostatin immunogens since different antigens vary in their immunogenicity to induce antibodies with unique binding specificities. Sera titers confirmed significant antibody levels in the immunized female mice and their maternal transfer to offspring. Myo-1 and Myo-2 sera showed greater affinities to their respective coating antigens than to rupMyo coating antigen, indicating the antigenic specificity of Myo-1 and Myo-2 peptides in eliciting antibodies with unique binding specificities. There was no significant cross-reactivity of Myo-1 sera to Myo-2 coating antigen or Myo-2 sera to Myo-1 coating antigen. The rMyo serum showed affinity to both Myo-1 and Myo-2 coating antigens, indicating that immunization with mature myostatin protein (rMyo) confers antibodies against both Myo-1 and Myo-2 peptide fragments as well, since rMyo immunogen contains both Myo-1 and Myo-2 antigenic sequences.

Interestingly, active immunization against myostatin appeared to affect fertility in the immunized female mice in our study as two mice in rMyo and one mouse, each in Myo-1 and Myo-2 groups did not conceive. However, the litter sizes from the treatment groups were not significantly different from the control litter size. In contrast to our results, Liang et al. (2007) observed significantly smaller litter size (3 pups / mouse) from the mice immunized with myostatin peptide (AA sequence from 313 to 323), compared to control litter size (7 pups / mouse). Furthermore, lesser number of ovarian follicles was observed in the immunized mice. Based on the above results, they speculated that myostatin might have a role in follicular development. They also proposed the possibility that the anti-myostatin antibody could have crossreacted with other TGF-β family members such as inhibin and GDF-9, which are involved in follicle development.

As expected, maternal transfer of antibodies was evident in 3-day old offsprings, with the antibody binding specificities being similar to those of their respective immunized mothers. Liang et al. (2007) reported the presence of maternally transferred anti-myostatin antibodies as long as 8 weeks post-partum in the offspring. Although we measured the sera titers only in 3-day old neonates, the aforementioned study suggests the possible presence of antibodies even up to 8 wks of age. However, we noticed a significant variability in the titers among littermates, which could be due to variations in titer levels in their respective mothers and/or variations in maternal antibody transfer process from animal to animal. In addition, the variable amounts of colostrum suckled by newborns may also affect the titer levels since immunoglobulins are also secreted in colostrum in significant amounts (Roberts et al., 1990; Ahouse et al., 1993). Even though we did not attempt to measure the antibody levels in the colostrum/milk in this study, it is

postulated that the maternally transferred antibodies in 3-day old neonates could have been transmitted through both placenta and/or colostrum.

Despite the evident maternal transfer of anti-myostatin antibodies to the offspring, no significant differences in the body weights were observed among the litters from the immunized mice until 8 wks post-partum. However, the gastrocnemius and triceps of the Myo-2 offspring were significantly heavier, while those of the rMyo and Myo-1 offspring did not differ from those of the control offspring. While, Liang et al. (2007) reported that active maternal immunization against myostatin, using a myostatin peptide (AA sequence from 313 to 323) in mice, enhanced growth rate, body crude protein content and decreased body fat content of offspring. Since the immunogen that was used in Liang's study was different from the myostatin immunogens used in our study, it was speculated that different types of myostatin immunogens produced antibodies with different binding affinities to myostatin and/or variable efficacies in suppressing myostatin activity, resulting in inconsistent responses in the growth rate and muscle mass of offspring.

Myostatin is produced as a prepropeptide composed of an N-terminal propeptide and a C-terminal mature domain (Mc Pherron et al., 1997). The C-terminal mature myostatin is released upon the removal of N-terminal propeptide by proteolysis at the conserved tetrabasic (RSRR) site (Lee and Mc Pherron, 2001). Mature myostatin protein, like many other TGF- β members, forms a homodimer that binds to *Act*RIIB receptors located on the muscle cells to initiate signal transduction (Lee and Mc Pherron, 2001). The binding of myostatin dimer to *Act*RIIB receptors induces activation of Smad2/3, the intracellular signal transducers, which translocates into the nucleus and interact with the Smad binding sequences in the promoter region of target genes to regulate their

expression (Rebbapragada et al., 2003). The sequence, AG (C/A) CAGACA, commonly called CAGA box was identified as the Smad binding site (Dennler et al., 1998). Based on this, a luciferase reporter system was developed with the CAGA box being inserted in the promoter region of a luciferase containing plasmid, which has been widely used to examine the biological activity of myostatin (Hill et al, 2002 and 2003; Zimmers et al., 2002; Thies et al., 200; Zhu et al., 2004).

To examine whether the antibodies of the Myo-2 group were different from those of rMyo and Myo-1 groups in their ability to suppress myostatin activity, we used the pGL3 $(CAGA)_{12}$-Luc-luciferase reporter system. We also examined the binding affinities of the antibodies to myostatin on Western blot analysis. Disappointedly, in the pGL3 $(CAGA)_{12}$-Luc-luciferase reporter assay system, none of the antibodies from the three immunized groups showed the ability to suppress myostatin's activity, demonstrating that the antibodies of the Myo-2 group were not different from those of the rMyo and Myo-1 groups in their ability to inhibit myostatin's activity. Furthermore, in Western blot analysis, the purified IgGs from all treatment groups (rMyo, Myo-1 and Myo-2) showed affinity to mature myostatin monomer, but none of them showed affinity to the myostatin dimer, supporting the luciferase assay result. Therefore, the results from the luciferase assay and Western blot analysis suggest that the increased muscle mass observed in the Myo-2 offspring was probably not resulted from an inhibitory action of anti-Myo-2 antibodies on myostatin. Currently, we have no data explaining why an increase in muscle mass occurred only in the Myo-2 offspring but not in the rMyo or Myo-1 groups. It, thus, was questioned whether the increase in muscle mass of the Myo-2 offspring was the true effect of maternal immunization using Myo-2. Since Liang et al. (2007) reported

that maternal immunization against myostatin peptide in mice enhanced growth rate and body protein gain in offspring; we compared the peptide sequence of their immunogen with the sequence of Myo-2. Interestingly, a significant portion of their peptide antigen overlapped with the Myo-2 antigen. The sequence of Liang's antigen was ECEFVFLQKYP and the Myo-2 sequence was VFLQKYPHTHLVHQA, revealing seven amino acids overlap between the two antigens. Taken together, we cannot rule out the possibility of the anti-Myo-2 antibodies capable of increasing muscle mass of the Myo-2 offspring through unidentified mechanism(s), independent of myostatin activity.

In conclusion, we observed that the active immunization against myostatin using Myo-2 peptide improved the muscle growth of offspring. However, the inability of the anti-Myo-2 antibody to bind mature myostatin dimer and to suppress the myostatin activity indicates that the improved muscle mass in the Myo-2 offspring was probably not due to the inhibition of myostatin's biological activity by the anti-Myo-2 antibodies, but yet unidentified action of the anti-Myo-2 antibodies on skeletal muscle growth. Therefore, further studies are needed to determine whether active immunization against myostatin has the potential to improve skeletal muscle growth of offspring.

REFERENCES

Adams TE, Daley CA, Adams BM and Sakurai H. Testis function and feedlot performance of bulls actively immunized against gonadotropin-releasing-hormone - Effect of implants containing progesterone and estradiol benzoate. *Journal of Animal Science* 71: 811-817, 1993.

Ahouse JJ, Hagerman CL, Mittal P, Gilbert DJ, Copeland NG, Jenkins NA and Simister NE. Mouse MHC class I-like Fc receptor encoded outside the MHC. *Journal of Immunology* 151: 6076-6088, 1993.

Amthor H, Huang RJ, McKinnell I, Christ B, Kambadur R, Sharma M and Patel K. The regulation and action of myostatin as a negative regulator of muscle development during avian embryogenesis. *Developmental Biology* 251: 241-257, 2002.

Amthor H, Nicholas G, McKinnell I, Kemp CF, Sharma M, Kambadur R and Patel K. Follistatin complexes myostatin and antagonizes myostatin-mediated inhibition of myogenesis. *Developmental Biology* 270: 19-30, 2004.

Artaza JN, Bhasin S, Mallidis C, Taylor W, Ma K and Gonzalez-Cadavid NF. Endogenous expression and localization of myostatin and its relation to myosin heavy chain distribution in C2C12 skeletal muscle cells. *Journal of Cellular Physiology* 190: 170-179, 2002.

Artaza JN, Bhasin S, Magee TR, Reisz-Porszasz S, Shen RQ, Groome NP, Fareez MM and Gonzalez-Cadavid NF. Myostatin inhibits myogenesis and promotes adipogenesis in C3H 10T(1/2) mesenchymal multipotent cells. *Endocrinology* 146: 3547-3557, 2005.

Attisano L and Wrana JL. Smads as transcriptional co-modulators. *Current Opinion in Cell Biology* 12: 235-243, 2000.

Berry C, Thomas M, Langley B, Sharma M and Kambadur R. Single cysteine to tyrosine transition inactivates the growth inhibitory function of Piedmontese myostatin. *American Journal of Physiology-Cell Physiology* 283: C135-C141, 2002.

Bogdanovich S, Krag TOB, Barton ER, Morris LD, Whittemore LA, Ahima RS and Khurana TS. Functional improvement of dystrophic muscle by myostatin blockade. *Nature* 420: 418-421, 2002.

Bradford MM. A rapid and sensitive method for the quantitation of microgram quantities of protein utilizing the principle of protein-dye binding. *Analytical Biochemistry* 72: 248-254, 1976.

Carlson CJ, Booth FW and Gordon SE. Skeletal muscle myostatin mRNA expression is fiber-type specific and increases during hindlimb unloading. *American Journal*

of Physiology-Regulatory Integrative and Comparative Physiology 277: R601-R606, 1999.

Dennler S, Itoh S, Vivien D, ten Dijke P, Huet S and Gauthier JM. Direct binding of Smad3 and Smad4 to critical TGF beta-inducible elements in the promoter of human plasminogen activator inhibitor-type 1 gene. *European Molecular Biology Organization Journal* 17: 3091-3100, 1998.

Derynck R and Feng XH. TGF-[beta] receptor signaling. *Biochimica et Biophysica Acta (BBA) - Reviews on Cancer* 1333: F105-F150, 1997.

Dunshea FR, Colantoni C, Howard K, McCauley I, Jackson P, Long KA, Lopaticki S, Nugent EA, Simons JA, Walker J and Hennessy DP. Vaccination of boars with a GnRH vaccine (Improvac) eliminates boar taint and increases growth performance. *Journal of Animal Science* 79: 2524-2535, 2001.

Feldman BJ, Streeper RS, Farese RV and Yamamoto KR. Myostatin modulates adipogenesis to generate adipocytes with favorable metabolic effects. *Proceedings of the National Academy of Sciences of the United States of America* 103: 15675-15680, 2006.

Ferrell RE, Conte V, Lawrence EC, Roth SM, Hagberg JM and Hurley BF. Frequent sequence variation in the human myostatin (GDF8) gene as a marker for analysis of muscle-related phenotypes. *Genomics* 62: 203-207, 1999.

Forbes D, Jackman M, Bishop A, Thomas M, Kambadur R and Sharma M. Myostatin auto-regulates its expression by feedback loop through Smad7 dependent mechanism. *Journal of Cellular Physiology* 206: 264-272, 2006.

Gitlin D and Morphis LG. Systems of materno-foetal transport of gamma G immunoglobulin in the mouse. *Nature* 223: 195-196, 1969.

Goldspink G. Biochemical and physiological changes associated with the postnatal development of the biceps brachii. *Comparative Biochemistry and Physiology* 7: 157-166, 1962.

Gonzalez-Cadavid NF, Taylor WE, Yarasheski K, Sinha-Hikim I, Ma K, Ezzat S, Shen RQ, Lalani R, Asa S, Mamita M, Nair G, Arver S and Bhasin S. Organization of the human myostatin gene and expression in healthy men and HIV-infected men with muscle wasting. *Proceedings of the National Academy of Sciences of the United States of America* 95: 14938-14943, 1998.

Grobet L, Martin LJR, Poncelet D, Pirottin D, Brouwers B, Riquet J, Schoeberlein A, Dunner S, Menissier F, Massabanda J, Fries R, Hanset R and Georges M. A deletion in the bovine myostatin gene causes the double-muscled phenotype in cattle. *Nature Genetics* 17: 71-74, 1997.

Grobet L, Poncelet D, Royo LJ, Brouwers B, Pirottin D, Michaux C, Menissier F, Zanotti M, Dunner S and Georges M. Molecular definition of an allelic series of mutations disrupting the myostatin function and causing double-muscling in cattle. *Mammalian Genome* 9: 210-213, 1998.

Grobet L, Pirottin D, Farnir F, Poncelet D, Royo LJ, Brouwers B, Christians E, Desmecht D, Coignoul F, Kahn R and Georges M. Modulating skeletal muscle mass by postnatal, muscle-specific inactivation of the myostatin gene. *Genesis* 35: 227-238, 2003.

Hill JJ, Davies MV, Pearson AA, Wang JH, Hewick RM, Wolfman NM and Qiu YC. The myostatin propeptide and the follistatin-related gene are inhibitory binding proteins of myostatin in normal serum. *Journal of Biological Chemistry* 277: 40735-40741, 2002.

Hill JJ, Qiu YC, Hewick RM and Wolfman NM. Regulation of myostatin in vivo by growth and differentiation factor-associated serum protein-1: A novel protein with protease inhibitor and follistatin domains. *Molecular Endocrinology* 17: 1144-1154, 2003.

Hirai S, Matsumoto H, Hino N, Kawachi H, Matsui T and Yano H. Myostatin inhibits differentiation of bovine preadipocyte. *Domestic Animal Endocrinology* 32: 1-14, 2007.

Holder AT, Aston R, Preece MA and Ivanyi J. Monoclonal antibody-mediated enhancement of growth-hormone activity *in vivo*. *Journal of Endocrinology* 107: R9-R12, 1985.

Holder AT, Aston R, Rest JR, Hill DJ, Patel N and Ivanyi J. Monoclonal-antibodies can enhance the biological-activity of thyrotropin. *Endocrinology* 120: 567-573, 1987.

Huxsoll CC, Price EO and Adams TE. Testis function, carcass traits, and aggressive behavior of beef bulls actively immunized against gonadotropin-releasing hormone. *Journal of Animal Science* 76: 1760-1766, 1998.

Israel EJ, Patel VK, Taylor SF, Marshakrothstein A and Simister N. Requirement for a beta(2)-microglobulin-associated Fc receptor for acquisition of maternal Igg by fetal and neonatal mice. *Journal of Immunology* 154: 6246-6251, 1995.

Israel EJ, Taylor S, Wu Z, Mizoguchi E, Blumberg RS, Bhan A and Simister NE. Expression of the neonatal Fc receptor, FcRn, on human intestinal epithelial cells. *Immunology* 92: 69-74, 1997.

Ji SQ, Losinski RL, Cornelius SG, Frank GR, Willis GM, Gerrard DE, Depreux FFS and Spurlock ME. Myostatin expression in porcine tissues: tissue specificity and developmental and postnatal regulation. *American Journal of Physiology-Regulatory Integrative and Comparative Physiology* 44: R1265-R1273, 1998.

Ji S, Willis GM, Cornelius SG, Frank GR and Spurlock ME. Porcine myostatin in muscle and mammary gland development. *Federation of American Societies for Experimental Biology Journal* 13: A415, 1999.

Jin HJ, Dunn MA, Borthakur D and Kim YS. Refolding and purification of unprocessed porcine myostatin expressed in Escherichia coli. *Protein Expression and Purification* 35: 1-10, 2004.

Joulia D, Bernardi H, Garandel W, Rabenoelina F, Vernus B and Cabello G. Mechanisms involved in the inhibition of myoblast proliferation and differentiation by myostatin. *Experimental Cell Research* 286: 263-275, 2003.

Joulia-Ekaza D and Cabello G. Myostatin regulation of muscle development: Molecular basis, natural mutations, physiopathological aspects. *Experimental Cell Research* 312: 2401-2414, 2006.

Kambadur R, Sharma M, Smith TPL and Bass JJ. Mutations in myostatin (GDF8) in double-muscled Belgian blue and Piedmontese cattle. *Genome Research* 7: 910-916, 1997.

Kawada S, Tachi C and Ishii N. Content and localization of myostatin in mouse skeletal muscles during aging, mechanical unloading and reloading. *Journal of Muscle Research and Cell Motility* 22: 627-633, 2001.

Kim HS, Liang L, Dean RG, Hausman DB, Hartzell DL and Baile CA. Inhibition of preadipocyte differentiation by myostatin treatment in 3T3-L1 cultures. *Biochemical and Biophysical Research Communications* 281: 902-906, 2001.

Kim YS, Bobbili NK, Paek KS and Jin HJ. Production of a monoclonal anti-myostatin antibody and the effects of in ovo administration of the antibody on posthatch broiler growth and muscle mass. *Poultry Science* 85: 1062-1071, 2006.

Kocamis H, Richter J, Klandorf H and Killefer J. The ontogeny of myostatin and follistatin mRNA expression during chicken embryonic development. *Federation of American Societies for Experimental Biology Journal* 13: A356, 1999.

Kocamis H, McFarland DC and Killefer J. Temporal expression of growth factor genes during myogenesis of satellite cells derived from the biceps femoris and pectoralis major muscles of the chicken. *Journal of Cellular Physiology* 186: 146-152, 2001.

Kohler PF and Farr RS. Elevation of cord over maternal IgG immunoglobulin: evidence for an active placental IgG transport. *Nature* 210: 1070-1071, 1966.

Laemmli UK. Cleavage of structural proteins during the assembly of the head of bacteriophage T4. *Nature* 227: 680-685, 1970.

Lalani R, Bhasin S, Byhower F, Tarnuzzer R, Grant M, Shen R, Asa S, Ezzat S and Gonzalez-Cadavid NF. Myostatin and insulin-like growth factor-I and -II expression in the muscle of rats exposed to the microgravity environment of the Neurolab space shuttle flight. *Journal of Endocrinology* 167: 417-428, 2000.

Lang CH, Silvis C, Nystrom G and Frost RA. Regulation of myostatin by glucocorticoids after thermal injury. *Federation of American Societies for Experimental Biology Journal* 15: 1807-1809, 2001.

Langley B, Thomas M, Bishop A, Sharma M, Gilmour S and Kambadur R. Myostatin inhibits myoblast differentiation by down-regulating MyoD expression. *Journal of Biological Chemistry* 277: 49831-49840, 2002.

Langley B, Thomas M, McFarlane C, Gilmour S, Sharma M and Kambadur R. Myostatin inhibits rhabdomyosarcoma cell proliferation through an Rb-independent pathway. *Oncogene* 23: 524-534, 2004.

Lee SJ and McPherron AC. Regulation of myostatin activity and muscle growth. *Proceedings of the National Academy of Sciences of the United States of America* 98: 9306-9311, 2001.

Lee SJ, Reed LA, Davies MV, Girgenrath S, Goad MEP, Tomkinson KN, Wright JF, Barker C, Ehrmantraut G, Holmstrom J, Trowell B, Gertz B, Jiang MS, Sebald SM, Matzuk M, Li E, Liang LF, Quattlebaum E, Stotish RL and Wolfman NM. Regulation of muscle growth by multiple ligands signaling through activin type II receptors. *Proceedings of the National Academy of Sciences of the United States of America* 102: 18117-18122, 2005.

Liang YC, Yeh JY and Ou BR. Effect of maternal myostatin antibody on offspring growth performance and body composition in mice. *Journal of Experimental Biology* 210: 477-483, 2007.

Lin J, Arnold HB, la-Fera MA, Azain MJ, Hartzell DL and Baile CA. Myostatin knockout in mice increases myogenesis and decreases adipogenesis. *Biochemical and Biophysical Research Communications* 291: 701-706, 2002.

Liu W, Thomas SG, Asa SL, Gonzalez-Cadavid N, Bhasin S and Ezzat S. Myostatin is a skeletal muscle target of growth hormone anabolic action. *Journal of Clinical Endocrinology and Metabolism* 88: 5490-5496, 2003.

Longsworth LG, Curtis RM and Pembroke RH. The electrophoretic analysis of maternal and fetal plasmas and sera. *Journal of Clinical Investigation* 24: 46-53, 1945.

Lowry OH, Rosebrough NJ, Farr AL and Randall RJ. Protein measurement with the Folin phenol reagent. *Journal of Biological Chemistry* 193: 265-275, 1951.

Ma K, Mallidis C, Artaza J, Taylor W, Gonzalez-Cadavid N and Bhasin S. Characterization of 5 '-regulatory region of human myostatin gene: regulation by dexamethasone in vitro. *American Journal of Physiology-Endocrinology and Metabolism* 281: E1128-E1136, 2001.

Ma K, Mallidis C, Bhasin S, Mahabadi V, Artaza J, Gonzalez-Cadavid N, Arias J and Salehian B. Glucocorticoid-induced skeletal muscle atrophy is associated with upregulation of myostatin gene expression. *American Journal of Physiology-Endocrinology and Metabolism* 285: E363-E371, 2003.

Maccatrozzo L, Bargelloni L, Cardazzo B, Rizzo G and Patarnello T. A novel second myostatin gene is present in teleost fish. *Federation of the Societies of Biochemistry and Molecular Biology Letters* 509: 36-40, 2001.

Magee TR, Artaza JN, Ferrini MG, Vernet D, Zuniga FI, Cantini L, Porszasz SR, Rajfer J and Gonzalez-Cadavid NF. Myostatin short interfering hairpin ribonucleic acid gene transfer increases muscle mass and reduces interstitial connective tissue. *Journal of Investigative Medicine* 54: 1171-1181, 2006.

Massague J. TGF- Signal Transduction. *Annual Review of Biochemistry* 67: 753-791, 1998.

Massague J and Gomis RR. The logic of TGF [beta] signaling. *Febs Letters* 580: 2811-2820, 2006.

McCauley I, Watt M, Suster D, Kerton DJ, Oliver WT, Harrell RJ and Dunshea FR. A GnRF vaccine (Improvac (R)) and porcine somatotropin (Reporcin (R)) have synergistic effects upon growth performance in both boars and gilts. *Australian Journal of Agricultural Research* 54: 11-20, 2003.

McPherron AC, Lawler AM and Lee SJ. Regulation of skeletal muscle mass in mice by a new TGF-beta superfamily member. *Nature* 387: 83-90, 1997.

McPherron AC and Lee SJ. Double muscling in cattle due to mutations in the myostatin gene. *Proceedings of the National Academy of Sciences of the United States of America* 94: 12457-12461, 1997.

McPherron AC and Lee SJ. Suppression of body fat accumulation in myostatin-deficient mice. *Journal of Clinical Investigation* 109: 595-601, 2002.

Mendler L, Zador E, Ver Heyen M, Dux L and Wuytack F. Myostatin levels in regenerating rat muscles and in myogenic cell cultures. *Journal of Muscle Research and Cell Motility* 21: 551-563, 2000.

Miyazono K, Hellman U, Wernstedt C and Heldin CH. Latent high molecular weight complex of transforming growth factor beta 1. Purification from human platelets and structural characterization. *Journal of Biological Chemistry* 263: 6407-6415, 1988.

Moss FP and Leblond CP. Satellite cells as the source of nuclei in muscles of growing rats. *Anatomical Records* 170: 421-435, 1971.

Nicholas G, Thomas M, Langley B, Somers W, Patel K, Kemp CF, Sharma M and Kambadur R. Titin-cap associates with, and regulates secretion of, myostatin. *Journal of Cellular Physiology* 193: 120-131, 2002.

Ostbye TK, Galloway TF, Nielsen C, Gabestad I, Bardal T and Andersen O. The two myostatin genes of Atlantic salmon (Salmo salar) are expressed in a variety of tissues. *European Journal of Biochemistry* 268: 5249-5257, 2001.

Peitsch MC, Wilkins MR, Tonella L, Sanchez JC, Appel RD and Hochstrasser DF. Large-scale protein modelling and integration with the SWISS-PROT and SWISS-2DPAGE databases: The example of Escherichia coli. *Electrophoresis* 18: 498-501, 1997.

Pekas JC and Trout WE. Stimulation of food-intake and growth of swine by cholecystokinin immunization. *Growth Development and Aging* 54: 51-56, 1990.

Pell JM and Aston R. Principles of Immunomodulation. *Livestock Production Science* 42: 123-133, 1995.

Pell JM. Immunological manipulation of growth. *Proceedings of the Nutrition Society* 56: 621-630, 1997.

Pirottin D, Grobet L, Adamantidis A, Farnir F, Herens C, Schroder HD and Georges M. Transgenic engineering of male-specific muscular hypertrophy. *Proceedings of the National Academy of Sciences of the United States of America* 102: 6413-6418, 2005.

Prendiville DJ, Enright WJ, Crowe MA, Finnerty M, Hynes N and Roche JF. Immunization of heifers against gonadotropin-releasing hormone: antibody titers, ovarian function, body growth, and carcass characteristics. *Journal of Animal Science* 73: 2382-2389, 1995.

Rayne J and Crawford GN. Increase in fibre numbers of the rat pterygoid muscles during postnatal growth. *Journal of Anatomy* 119: 1975.

Reardon KA, Davis J, Kapsa RMI, Choong P and Byrne E. Myostatin, insulin-like growth factor-1, and leukemia inhibitory factor mRNAs are upregulated in chronic human disuse muscle atrophy. *Muscle & Nerve* 24: 893-899, 2001.

Rebbapragada A, Benchabane H, Wrana JL, Celeste AJ and Attisano L. Myostatin signals through a transforming growth factor beta-like signaling pathway to block adipogenesis. *Molecular and Cellular Biology* 23: 7230-7242, 2003.

Reisz-Porszasz S, Bhasin S, Artaza JN, Shen RQ, Sinha-Hikim I, Hogue A, Fielder TJ and Gonzalez-Cadavid NF. Lower skeletal muscle mass in male transgenic mice with muscle-specific overexpression of myostatin. *American Journal of Physiology-Endocrinology and Metabolism* 285: E876-E888, 2003.

Rios R, Carneiro I, Arce VM and Devesa J. Myostatin regulates cell survival during C2C12 myogenesis. *Biochemical and Biophysical Research Communications* 280: 561-566, 2001.

Rios R, Carneiro I, Arce VM and Devesa J. Myostatin is an inhibitor of myogenic differentiation. *American Journal of Physiology-Cell Physiology* 282: C993-C999, 2002.

Roberts DM, Guenthert M and Rodewald R. Isolation and characterization of the Fc receptor from the fetal yolk-sac of the rat. *Journal of Cell Biology* 111: 1867-1876, 1990.

Roberts SB and Goetz FW. Differential skeletal muscle expression of myostatin across teleost species, and the isolation of multiple myostatin isoforms. *Federation of the Societies of Biochemistry and Molecular Biology Letters* 491: 212-216, 2001.

Rodgers BD, Weber GM, Sullivan CV and Levine MA. Isolation and characterization of myostatin complementary deoxyribonucleic acid clones from two commercially important fish: Oreochromis mossambicus and Morone chrysops. *Endocrinology* 142: 1412-1418, 2001.

Rowe RWD. The effect of hypertrophy on the properties of skeletal muscle. *Comparative Biochemistry and Physiology* 28: 1449-1453, 1969.

Sakuma K, Watanabe K, Sano M, Uramoto I and Totsuka T. Differential adaptation of growth and differentiation factor 8/myostatin, fibroblast growth factor 6 and leukemia inhibitory factor in overloaded, regenerating and denervated rat muscles. *Biochimica et Biophysica Acta-Molecular Cell Research* 1497: 77-88, 2000.

Sazanov A, Ewald D, Buitkamp J and Fries R. A molecular marker for the chicken myostatin gene (GDF8) maps to 7p11. *Animal Genetics* 30: 388-389, 1999.

Schuelke M, Wagner KR, Stolz LE, Hubner C, Riebel T, Komen W, Braun T, Tobin JF and Lee SJ. Brief report - Myostatin mutation associated with gross muscle hypertrophy in a child. *New England Journal of Medicine* 350: 2682-2688, 2004.

Schultz E. Satellite cell proliferative compartments in growing skeletal muscles. *Developmental Biology* 175: 84-94, 1996.

Sharma M, Kambadur R, Matthews BG, Somers WG, Devlin GP, Conaglen JV, Fowke PJ and Bass JJ. Myostatin, a transforming growth factor-beta superfamily member, is expressed in heart muscle and is upregulated in cardiomyocytes after infarct. *Journal of Cellular Physiology* 180: 1-9, 1999.

Sillence MN, Jones MR, Lowry P and Bassett JR. Passive immunization with antiserum to adrenocorticotropin increases weight gain in normal female rats. *Journal of Animal Science* 70: 1382-1388, 1992.

Simister NE and Rees AR. Isolation and Characterization of An Fc Receptor from Neonatal Rat Small-Intestine. *European Journal of Immunology* 15: 733-738, 1985.

Simister NE, Story CM, Chen HL and Hunt JS. An IgG-transporting Fc receptor expressed in the syncytiotrophoblast of human placenta. *European Journal of Immunology* 26: 1527-1531, 1996.

Simister NE. Placental transport of immunoglobulin G. *Vaccine* 21: 3365-3369, 2003.

Simpson-Morgan MW and Smeaton TC. The transfer of antibodies by neonates and adults. *Advances in Veterinary Science - Comparative Medicine* 16: 355-386, 1972.

Siriett V, Platt L, Salerno MS, Ling N, Kambadur R and Sharma M. Prolonged absence of myostatin reduces sarcopenia. *Journal of Cellular Physiology* 209: 866-873, 2006.

Sonstegard TS, Kappes SM, Keele JW and Smith TPL. Refinement of bovine chromosome 2 linkage map near the mh locus reveals rearrangements between the bovine and human genomes. *Animal Genetics* 29: 341-347, 1998[a].

Sonstegard TS, Rohrer GA and Smith TPL. Myostatin maps to porcine chromosome 15 by linkage and physical analyses. *Animal Genetics* 29: 19-22, 1998[b].

Spencer GSG, Garssen GJ and Hart IC. A novel-approach to growth promotion using auto-immunization against somatostatin .1. Effects on Growth and Hormone Levels in Lambs. *Livestock Production Science* 10: 25-37, 1983.

Spencer GS. Immunization against cholecystokinin decreases appetite in lambs. *Journal of Animal Science* 70: 3820-3824, 1992.

Stewart CE, Bates PC, Calder TA, Woodall SM and Pell JM. Potentiation of insulin-like growth factor-I (IGF-I) activity by an antibody: supportive evidence for enhancement of IGF-I bioavailability in vivo by IGF binding proteins. *Endocrinology* 133: 1462-1465, 1993.

Stratil A and Kopecny M. Genomic organization, sequence and polymorphism of the porcine myostatin (GDF8; MSTN) gene. *Animal Genetics* 30: 468-470, 1999.

Swatland HJ. Effect of growth and plane of nutrition on apparent muscle fiber numbers in the pig. *Growth* 40: 285-292, 1976.

Szabo G, Dallmann G, Muller G, Patthy L, Soller M and Varga L. A deletion in the myostatin gene causes the compact (Cmpt) hypermuscular mutation in mice. *Mammalian Genome* 9: 671-672, 1998.

Taylor WE, Bhasin S, Artaza J, Byhower F, Azam M, Willard DH, Kull FC and Gonzalez-Cadavid N. Myostatin inhibits cell proliferation and protein synthesis in C2C12 muscle cells. *American Journal of Physiology-Endocrinology and Metabolism* 280: E221-E228, 2001.

Thies RS, Chen T, Davies MV, Tomkinson KN, Pearson AA, Shakey QA and Wolfman NM. GDF-8 propeptide binds to GDF-8 and antagonizes biological activity by inhibiting GDF-8 receptor binding. *Growth Factors* 18: 251-259, 2001.

Thomas M, Langley B, Berry C, Sharma M, Kirk S, Bass J and Kambadur R. Myostatin, a negative regulator of muscle growth, functions by inhibiting myoblast proliferation. *Journal of Biological Chemistry* 275: 40235-40243, 2000.

Van de Perre P. Transfer of antibody via mother's milk. *Vaccine* 21: 3374-3376, 2003.

Wakefield LM, Smith DM, Flanders KC and Sporn MB. Latent transforming growth factor-beta from human platelets. A high molecular weight complex containing precursor sequences. *Journal of Biological Chemistry* 263: 7646-7654, 1988.

Wehling M, Cai BY and Tidball JG. Modulation of myostatin expression during modified muscle use. *Federation of American Societies for Experimental Biology Journal* 14: 103-110, 2000.

Whittemore LA, Song KN, Li XP, Aghajanian J, Davies M, Girgenrath S, Hill JJ, Jalenak M, Kelley P, Knight A, Maylor R, O'Hara D, Pearson A, Quazi A, Ryerson S, Tan XY, Tomkinson KN, Veldman GM, Widom A, Wright JF, Wudyka S, Zhao L and Wolfman NM. Inhibition of myostatin in adult mice increases skeletal muscle mass and strength. *Biochemical and Biophysical Research Communications* 300: 965-971, 2003.

Wigmore PM and Stickland NC. Muscle development in large and small pig fetuses. *Journal of Anatomy* 137: 235-245, 1983.

Wolfman NM, McPherron AC, Pappano WN, Davies MV, Song K, Tomkinson KN, Wright JF, Zhao L, Sebald SM, Greenspan DS and Leet SI. Activation of latent myostatin by the BMP-1/tolloid family of metalloproteinases. *Proceedings of the National Academy of Sciences of the United States of America* 100: 15842-15846, 2003.

Yamanouchi K, Soeta C, Naito K and Tojo H. Expression of myostatin gene in regenerating skeletal muscle of the rat and its localization. *Biochemical and Biophysical Research Communications* 270: 510-516, 2000.

Yang JZ, Ratovitski T, Brady JP, Solomon MB, Wells KD and Wall RJ. Expression of myostatin pro domain results in muscular transgenic mice. *Molecular Reproduction and Development* 60: 351-361, 2001.

Yang JZ and Zhao BP. Postnatal expression of myostatin propeptide cDNA maintained high muscle growth and normal adipose tissue mass in transgenic mice fed a high-fat diet. *Molecular Reproduction and Development* 73: 462-469, 2006.

Zagury D, Le Buanec H, Bizzini B, Burny A, Lewis G and Gallo RC. Active versus passive anti-cytokine antibody therapy against cytokine-associated chronic diseases. *Cytokine & Growth Factor Reviews* 14: 123-137, 2003.

Zagury D and Gallo RC. Anti-cytokine Ab immune therapy: present status and perspectives. *Drug Discovery Today* 9: 72-81, 2004.

Zhao BQ, Wall RJ and Yang JZ. Transgenic expression of myostatin propeptide prevents diet-induced obesity and insulin resistance. *Biochemical and Biophysical Research Communications* 337: 248-255, 2005.

Zhu HJ and Burgess AW. Regulation of transforming growth factor-[beta] signaling. *Molecular Cell Biology Research Communications* 4: 321-330, 2001.

Zhu XY, Topouzis S, Liang LF and Stotish RL. Myostatin signaling through Smad2, Smad3 and Smad4 is regulated by the inhibitory Smad7 by a negative feedback mechanism. *Cytokine* 26: 262-272, 2004.

Zimmers TA, Davies MV, Koniaris LG, Haynes P, Esquela AF, Tomkinson KN, McPherron AC, Wolfman NM and Lee SJ. Induction of cachexia in mice by systemically administered myostatin. *Science* 296: 1486-1488, 2002.

Zinkernagel RM. Maternal Antibodies, Childhood infections, and autoimmune diseases. *New England Journal of Medicine* 345: 1331-1335, 2001.

Table 2.1. Sera titer dynamics of immunized female mice

Treatment	After 1st Immunization	After 1st booster	After 2nd booster
	Against rupMyo coating antigen		
Control	$0.002^{a} \pm 0.0021$	$0.002^{a} \pm 0.0019$	$0.002^{a} \pm 0.0020$
rMyo	$0.132^{b} \pm 0.0079$	$0.192^{b} \pm 0.0230$	$0.314^{b} \pm 0.1004$
Myo-1	$0.277^{b} \pm 0.0910$	$0.433^{c} \pm 0.0177$	$0.535^{c} \pm 0.0267$
Myo-2	$0.076^{a} \pm 0.0052$	$0.161^{b} \pm 0.1186$	$0.222^{b} \pm 0.0053$
	Against Myo-1 coating antigen		
Control	0.005 ± 0.0031	$0.001^{a} \pm 0.0012$	$0.002^{a} \pm 0.0018$
rMyo	0.001 ± 0.0020	$0.171^{b} \pm 0.0023$	$0.397^{b} \pm 0.1405$
Myo-1	0.013 ± 0.0087	$0.183^{b} \pm 0.0076$	$0.573^{c} \pm 0.0532$
Myo-2	0.007 ± 0.0002	$0.006^{a} \pm 0.0004$	$0.196^{b} \pm 0.0531$
	Against Myo-2 coating antigen		
Control	0.002 ± 0.0011	$0.001^{a} \pm 0.0008$	$0.002^{a} \pm 0.0009$
rMyo	0.006 ± 0.0015	$0.001^{a} \pm 0.0055$	$0.037^{a} \pm 0.0303$
Myo-1	0.004 ± 0.0006	$0.016^{a} \pm 0.0061$	$0.062^{a} \pm 0.0249$
Myo-2	0.005 ± 0.0032	$0.097^{b} \pm 0.0376$	$0.302^{b} \pm 0.0406$

Sera titers were monitored at 2 wks following primary immunization and at each booster using ELISA. The data represent the average OD of duplicates at 405 nm ± SEM corrected to non-antigen coated control well readings from 1:250 sera dilution. Three different coating antigens used: rupMyo, a recombinant unprocessed porcine myostatin, Myo-1-BSA conjugate and Myo-2-BSA conjugate. Mean differences were analyzed by the Tukeys-HSD test. Means not sharing the same superscript in the same column differ at $P<0.05$.

Table 2.2. Sera titers of immunized female mice prior to breeding

Group	Coating antigen		
	rupMyo	Myo-1	Myo-2
Control (n=5)	$0.002^{a} \pm 0.0018$	$0.001^{a} \pm 0.0010$	$0.001^{a} \pm 0.0008$
rMyo (n=5)	$0.228^{b} \pm 0.0116$	$0.165^{a} \pm 0.0047$	$0.057^{a} \pm 0.0199$
Myo-1 (n=5)	$0.526^{c} \pm 0.0224$	$0.410^{b} \pm 0.1096$	$0.008^{a} \pm 0.0012$
Myo-2 (n=5)	$0.302^{b} \pm 0.0363$	$0.008^{a} \pm 0.0018$	$0.573^{b} \pm 0.0475$

The data represent the average OD of duplicates at 405 nm ± SEM corrected to non-antigen coated control well readings from 1:250 sera dilution. Titers represent the anti-myostatin antibody levels in the immunized female mice just before breeding. Three different coating antigens used: rupMyo, a recombinant unprocessed porcine myostatin, Myo-1-BSA conjugate and Myo-2-BSA conjugate. Mean differences were analyzed by the Tukeys-HSD test. Means not sharing the same superscript in the same column differ at $P<0.05$.

Table: 2.3. Body weights of immunized female mice during immunization regimen

Body weight (gm)	Treatment groups (Active Immunizations)				
	Con (n=5)	rMyo (n=5)	Myo-1 (n=5)	Myo-2 (n=5)	Statistical analysis
0 Wk	**21.03** (0.335)	**21.00** (0.276)	**20.80** (0.554)	**21.03** (0.603)	**NS**
1 Wk	**22.04** (0.322)	**21.19** (0.350)	**21.47** (0.552)	**21.74** (0.712)	**NS**
2 Wk	**22.84** (0.336)	**21.80** (0.336)	**21.76** (0.409)	**22.26** (0.653)	**NS**
3 Wk	**23.21** (0.476)	**22.31** (0.163)	**22.02** (0.593)	**23.60** (0.726)	**NS**
4 Wk	**22.92** (0.631)	**22.60** (0.188)	**22.07** (0.488)	**23.88** (1.098)	**NS**
5 Wk	**22.68** (0.447)	**22.79** (0.502)	**22.41** (0.741)	**23.08** (0.722)	**NS**
6 Wk	**23.68** (0.537)	**22.40** (0.250)	**22.24** (0.474)	**23.56** (1.022)	**NS**
7 Wk	**23.48** (0.655)	**23.02** (0.600)	**22.41** (0.390)	**24.23** (0.858)	**NS**

Data are least square means (SEM). NS, No Significance. Body wts were monitored starting from the primary immunization (0 Wk) and every week thereafter until the mice were bred.

Table 2.4. Sera titers of 3-day old neonates from immunized female mice

	Coating antigen		
Group	**rupMyo**	**Myo-1**	**Myo-2**
Control (n=5)	$0.010^{a} \pm 0.0097$	$0.002^{a} \pm 0.0009$	$0.003^{a} \pm 0.0010$
rMyo (n=3)	$0.076^{ab} \pm 0.0676$	$0.001^{a} \pm 0.0018$	$0.001^{a} \pm 0.0006$
Myo-1 (n=4)	$0.245^{b} \pm 0.0539$	$0.049^{b} \pm 0.0120$	$0.050^{ab} \pm 0.0142$
Myo-2 (n=4)	$0.053^{a} \pm 0.0357$	$0.043^{b} \pm 0.0124$	$0.178^{b} \pm 0.0701$

The data represent the average OD of duplicates at 405 nm ± SEM corrected to non-antigen coated control well readings from 1:250 sera dilution. Three different coating antigens used: rupMyo, a recombinant unprocessed porcine myostatin, Myo-1-BSA conjugate and Myo-2-BSA conjugate. Mean differences were analyzed by the Tukeys-HSD test. Means not sharing the same superscript in the same column differ at $P<0.05$.

Table: 2.5. Body weights of offspring from immunized female mice until 8 wks of age[1]

Body weight	Treatment[1]				Sex[1]		Significance		
	Control (n=40)	rMyo (n=19)	Myo-1 (n=28)	Myo-2 (n=30)	Male (n=53)	Female (n=60)	Trt	Sex	Trt X Sex
1 Wk	3.95 (0.203)	4.15 (0.262)	4.55 (0.227)	4.198 (0.203)	-	-	NS	-	-
2 Wk	7.09 (0.178)	6.89 (0.231)	7.56 (0.200)	7.53 (0.178)	-	-	NS	-	-
3 Wk	9.51 (0.410)	9.13 (0.529)	10.29 (0.458)	9.82 (0.410)	-	-	NS	-	-
4 Wk	15.30 (0.602)	14.53 (0.832)	14.49 (1.001)	14.76 (0.574)	15.67[a] (0.443)	13.87[b] (0.436)	NS	**	NS
5 Wk	18.00 (0.478)	18.02 (0.657)	17.66 (0.525)	18.30 (0.457)	19.74[a] (0.342)	16.25[b] (0.330)	NS	**	NS
6 Wk	19.37 (0.455)	19.39 (0.636)	18.50 (0.508)	19.58 (0.432)	21.36[a] (0.331)	17.06[b] (0.326)	NS	**	NS
7 Wk	20.70 (0.626)	20.08 (0.859)	20.06 (0.681)	20.67 (0.590)	22.84[a] (0.453)	17.92[b] (0.446)	NS	**	NS
8 Wk	20.44 (0.245)	20.49 (0.398)	20.73 (0.383)	21.42 (0.289)	23.57[a] (0.251)	17.97[b] (0.223)	+	***	NS

Data are least square means (SEM). ***, P<0.001; **, P<0.01; +, P<0.1; NS, Not Significant

[1]Mean differences were analyzed by Tukeys-HSD test; means not sharing the same superscript differ at P<0.05

Littermates from each immunized female mouse were weighed collectively until weaned at 3rd wk. Between 4 to 7 wks male, female littermates were weighed separately, and at 8th wk (sacrifice) litters were weighed individually.

Table: 2.6. Carcass characteristics of offspring upon sacrifice (8 Wks)[1]

Parameter	Treatment[1]				Sex		Significance		
	Con	rMyo	Myo-1	Myo-2	Male	Female	Treatment	Sex	Trt X Sex
Carcass wt, g	7.46 (0.104)	7.43 (0.167)	7.68 (0.160)	7.81 (0.118)	8.84[a] (0.104)	6.35[b] (0.094)	NS	***	NS
Carcass %	36.36 (0.234)	36.10 (0.374)	36.86 (0.359)	36.37 (0.265)	37.49[a] (0.233)	35.34[b] (0.210)	NS	***	NS
Gas complex[2], mg	109.98[a] (1.964)	107.96[a] (3.143)	115.08[ab] (3.015)	119.61[b] (2.223)	135.45[a] (1.956)	90.86[b] (1.767)	**	***	NS
Gas complex %[3]	0.53[a] (0.007)	0.52[a] (0.011)	0.55[a] (0.010)	0.56[a] (0.007)	0.57[a] (0.007)	0.50[b] (0.006)	*	***	NS
Triceps, mg	71.71[a] (1.423)	70.49[a] (2.289)	73.05[a] (2.194)	80.29[b] (1.621)	86.92[a] (1.423)	60.86[b] (1.286)	***	***	NS
Triceps %[3]	0.35[a] (0.005)	0.34[a] (0.008)	0.35[a] (0.007)	0.37[b] (0.005)	0.37[a] (0.005)	0.34[b] (0.004)	***	***	NS
Visceral fat, mg	140.34[a] (9.440)	149.09[ab] (15.105)	144.54[ab] (14.492)	178.24[b] (10.705)	207.95[a] (9.400)	98.15[b] (8.492)	*	***	**
Visceral fat %[3]	0.64 (0.041)	0.72 (0.065)	0.68 (0.063)	0.79 (0.046)	0.88[a] (0.041)	0.54[b] (0.037)	NS	***	**
Back fat[4], mg	133.18 (12.952)	105.13 (20.724)	104.82 (19.888)	120.52 (14.687)	125.79 (12.897)	106.03 (11.651)	NS	NS	NS
Back fat %[3]	0.66 (0.070)	0.51 (0.111)	0.50 (0.107)	0.56 (0.079)	0.53 (0.069)	0.59 (0.062)	NS	NS	NS

Data are least square means (SEM). ***, P<0.001; **, P<0.01; *, P<0.05; +, P<0.1.
[1]Means were compared by Tukeys-HSD test: means not sharing same superscript differ at P<0.05.
[2]Gastrocnemius complex includes gastrocnemius, plantaris and soleus. [3]The muscle or fat % is relative to body weight.

Table: 2.7. Visceral fat and visceral fat %[2] by sex in each treatment

Parameter	Males[1]				Females[1]			
	Control	rMyo	Myo-1	Myo-2	Control	rMyo	Myo-1	Myo-2
Visceral fat	**218.87^{a}** (11.942)	**173.00^{b}** (18.500)	**183.36^{ab}** (26.163)	**256.59^{c}** (15.635)	**61.82^{a}** (14.626)	**125.18^{b}** (23.884)	**105.72^{b}** (12.473)	**99.91^{c}** (14.626)
Visceral fat %	**0.92^{a}** (0.052)	**0.76^{b}** (0.080)	**0.77^{ab}** (0.113)	**1.05^{a}** (0.068)	**0.35^{a}** (0.063)	**0.69^{b}** (0.104)	**0.60^{b}** (0.054)	**0.54^{b}** (0.063)

Data are least square means (SEM).
[1]Means were compared by Tukeys-HSD test: means not sharing same superscript differ at $P<0.05$.
[2]The muscle or fat % is relative to body weight.

rMYO (RECOMBINANT MATURE MYOSTATIN):

LEVRVTDT PK**RSRR**DFGL D<u>C</u>DEHSTESR <u>CC</u>RYPLTVDF EAFGWDWIIA PKRYKANY<u>C</u>S GE<u>C</u>EF**VFLQK YPHTHLVHQA** NPRGSAGP<u>CC</u> TPTK**MSPINM LYFNGKEQII YGKIPAMV**VD R<u>C</u>G<u>C</u>S

MYO-1 PEPTIDE CONJUGATED TO KLH:

KLH (CG) MSP INM LYF NGK EQI IYG KIP AMV –OH

MYO-2 PEPTIDE CONJUGATED TO KLH:

KLH (CG) V FLQ KYP HTH LVH QA –OH

Figure 2.1. Amino acid sequences of three myostatin immunogens. The rMyo is a recombinant C-terminal mature myostatin protein with conserved proteolytic processing site that is shown in bold orange characters while the conserved cysteine residues in the C-terminal region are underlined in small characters. Fragments in highlighted blue-bold letters in the C-terminal mature myostatin signify the position of the Myo-2 (50 to 64) and Myo-1 (79 to 102) peptides on the mature domain, respectively. The rMyo was expressed in *E.coli* expression system in our lab previously (Kim et al., 2006), while Myo-1 and Myo-2 peptides were commercially synthesized and conjugated to keyhole limpet hemocyanin (KLH). A cysteine-glycine sequence was inserted at the N-terminal side of the peptides during synthesis to make a thio-ether linkage during the conjugation to carrier proteins. LC-SMCC (Pierce, Rockford, IL), a sulfhydryl- and amine-reactive heterobifunctional cross-linking agent, was used for conjugation of peptides to the carrier protein.

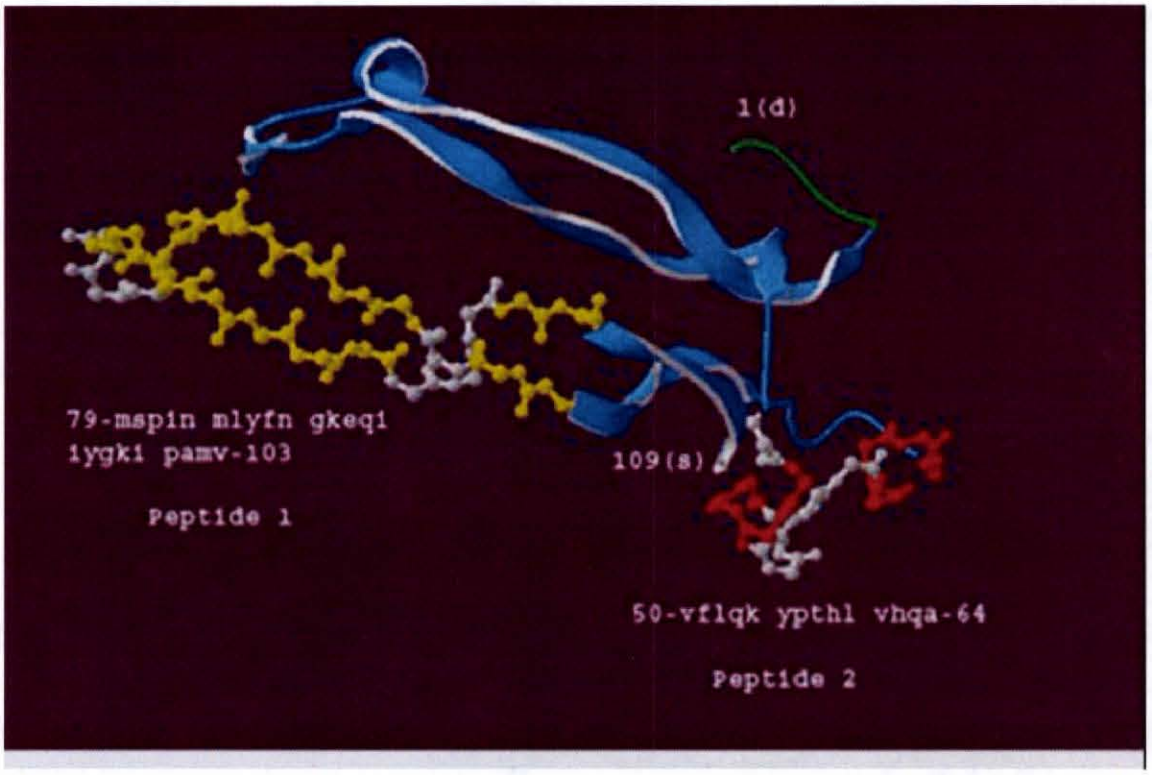

Figure 2.2. 3-D model of mature myostatin monomer. The figure is a model of C-terminal active/mature myostatin monomer, and rMyo immunogen is a denatured recombinant mature myostatin dimer. Myo-1 and Myo-2 peptides are highlighted in yellow and red, respectively. The structural model was generated using the SWISS-MODEL repository (Peitsch et al., 1997)

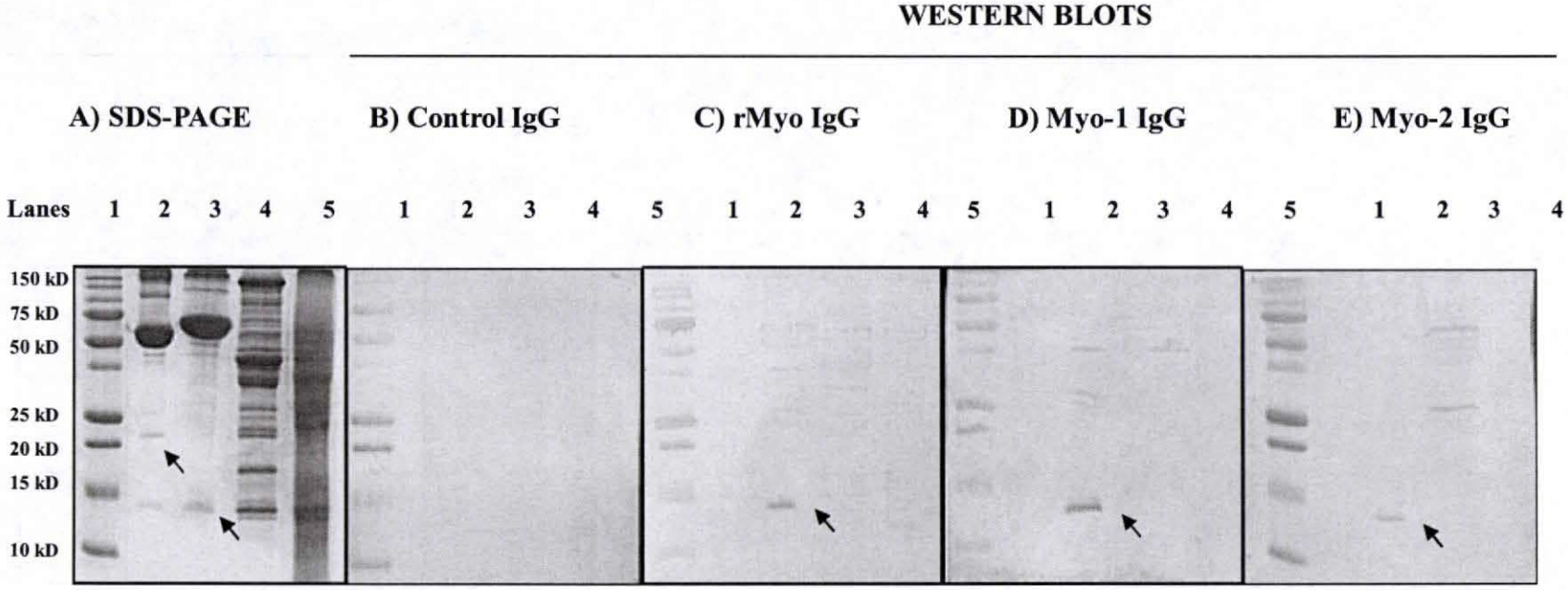

Figure 2.3. Binding characteristics of affinity-purified antibodies to myostatin. Molecular wt standard (lane 1), 200 ng of mature myostatin in non-reduced (lane 2), reduced (lane 3) condition, 4 μg of leg muscle (lane 4) and liver tissue homogenate (lane 5) were fractionated on 15% SDS-PAGE and visualized with Coomassie blue stain (A) or electrophoretically transferred onto a PVDF membrane (B to E). The membranes were incubated with 2 µg/ml affinity-purified IgG from Control (B), rMyo (C), Myo-1 (D) and Myo-2 (E) groups. Secondary anti-mouse antibody conjugated to alkaline phosphate was added at 1: 10,000 dilution. Images were captured by Multimager (Bio-Rad, Hercules, CA). Upper and lower arrows point the myostatin dimer and monomer, respectively.

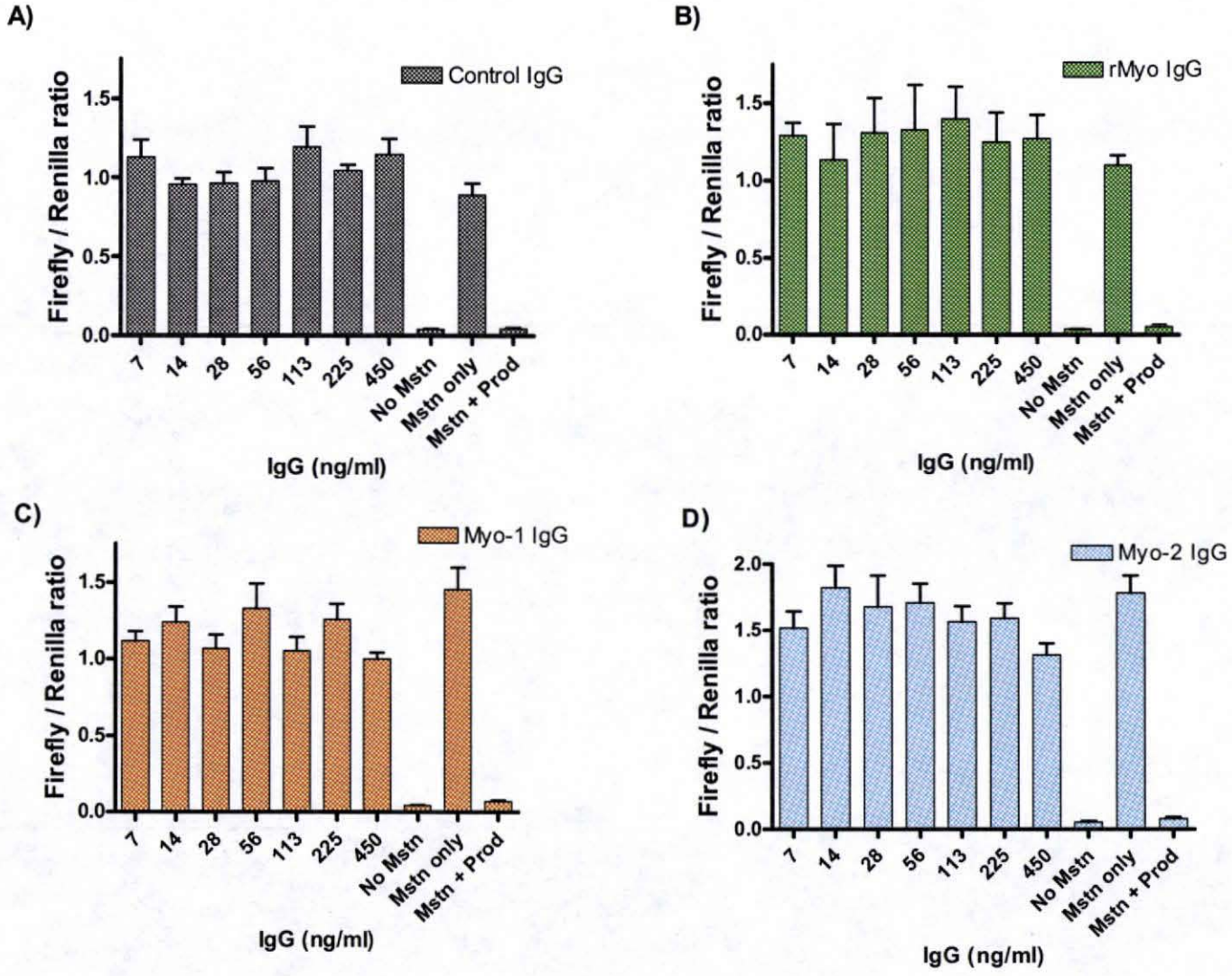

Figure 2.4. Effects of affinity-purified antibodies on myostatin's activity in pGL3 $(CAGA)_{12}$ Luc-luciferase reporter system

Figure 2.4. Effects of affinity-purified IgG on myostatin's activity in pGL3 $(CAGA)_{12}$ Luc-luciferase reporter system. A204 cells were seeded (40,000 cells/ml) on a 96-well culture plate and grown on DMEM with 10% fetal calf serum, antibiotic and antimycotic. After 36 hours, a mixture containing 0.2 μg of pGL3 $(CAGA)_{12}$ Luc-luciferase plasmid, 0.05 μg of pRL-TK- Renilla luciferase plasmid and 0.5 μl of lipofectamine 2000 in antibiotic-free DMEM containing 10% FCS . After 24 hours of transfection, the cells were serum starved for 9 hours. After serum starvation, myostatin (5 ng/ml) and various dilutions of the affinity-purified IgGs were added to each well in quadruplets followed by incubation for 6-8 hours. Luciferase activity was measured by Veritas microplate luminometer (Turner Biosystems Inc, CA) using two different substrates for firefly and renilla luciferase enzymes. Figures A, B, C and D bar diagrams represent the ratios of firefly luciferase to renilla luciferase in affinity-purified IgG treated wells from control, rMyo, Myo-1 and Myo-2, respectively. Positive controls were maintained on 5 ng/ml myostatin and 30 ng/ml prodomain while negative controls were on 5 ng/ml myostatin, without prodomain.

APPENDIX 1

Summary of sera titers of immunized female mice prior to breeding

Treatment	Coating antigen	Serum dilution				
		250	625	1563	3906	9766
Control	**rupMyo**	**0.002** (0.0019)	**0.001** (0.0006)	**0.002** (0.0001)	**0.001** (0.0007)	**0.001** (0.0005)
	Myo-1	**-0.001** (0.0027)	**0.003** (0.0031)	**0.001** (0.0029)	**0.002** (0.0030)	**0.001** (0.0030)
	Myo-2	**-0.001** (0.0008)	**0.003** (0.0024)	**0.003** (0.0020)	**-0.001** (0.0009)	**0.000** (0.0012)
rMyo	**rupMyo**	**0.228** (0.0116)	**0.186** (0.0202)	**0.063** (0.0049)	**0.031** (0.0020)	**0.005** (0.0008)
	Myo-1	**0.165** (0.0047)	**0.130** (0.0043)	**0.044** (0.0071)	**0.007** (0.0047)	**0.000** (0.0014)
	Myo-2	**0.057** (0.0199)	**0.041** (0.0139)	**0.024** (0.0093)	**0.012** (0.0035)	**0.015** (0.0018)
Myo-1	**rupMyo**	**0.526** (0.0224)	**0.343** (0.0210)	**0.203** (0.0066)	**0.061** (0.0030)	**0.006** (0.0048)
	Myo-1	**0.410** (0.1096)	**0.317** (0.1137)	**0.199** (0.0907)	**0.003** (0.0058)	**0.001** (0.0034)
	Myo-2	**0.008** (0.0018)	**0.003** (0.0023)	**0.005** (0.0031)	**0.003** (0.0010)	**0.004** (0.0010)
Myo-2	**rupMyo**	**0.302** (0.0363)	**0.240** (0.0356)	**0.160** (0.0359)	**0.026** (0.0098)	**0.021** (0.0077)
	Myo-1	**0.008** (0.0018)	**0.003** (0.0023)	**0.005** (0.0031)	**0.003** (0.0010)	**0.004** (0.0010)
	Myo-2	**0.573** (0.0475)	**0.462** (0.0592)	**0.318** (0.0601)	**0.001** (0.0033)	**0.006** (0.0013)

The data represent the average OD of duplicates at 405 nm ± SEM corrected to non-antigen coated control well readings from 1:250 sera dilution. Titers represent the anti-myostatin antibody levels in the immunized female mice just before breeding, thus some mice received more than 2 boosters based on the titer levels. Three different coating antigens used: rupMyo, a recombinant unprocessed porcine myostatin, Myo-1-BSA conjugate and Myo-2-BSA conjugate.

APPENDIX 2

A) Sera titer curves of immunized female mice using rupMyo as a coating antigen

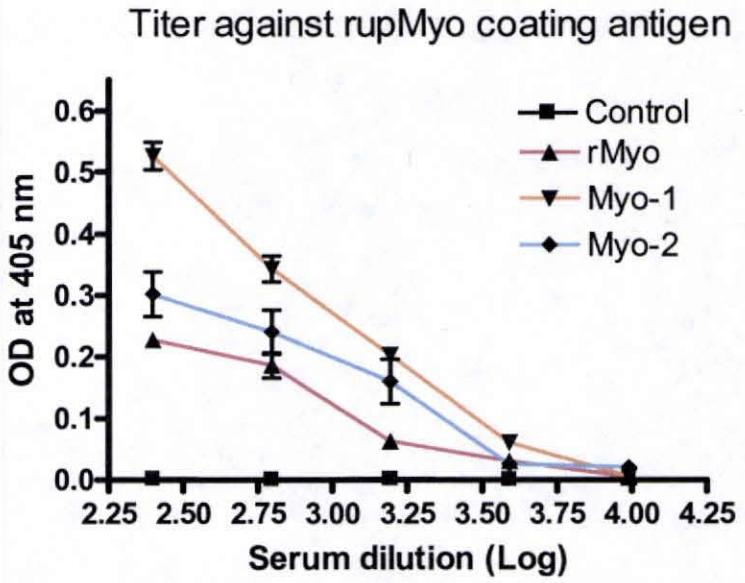

	Serum dilution				
Treatment	**250**	**625**	**1563**	**3906**	**9766**
Control	**0.002** (0.0019)	**0.001** (0.0006)	**0.002** (0.00017)	**0.001** (0.0007)	**0.001** (0.0005)
rMyo	**0.228** (0.0116)	**0.186** (0.0202)	**0.063** (0.0049)	**0.031** (0.0020)	**0.005** (0.0008)
Myo-1	**0.526** (0.0224)	**0.343** (0.0210)	**0.203** (0.0066)	**0.061** (0.0030)	**0.006** (0.0048)
Myo-2	**0.302** (0.0363)	**0.240** (0.0356)	**0.160** (0.0359)	**0.026** (0.0098)	**0.021** (0.0077)

B) Sera titer curves of immunized female mice using Myo-1-BSA as a coating antigen

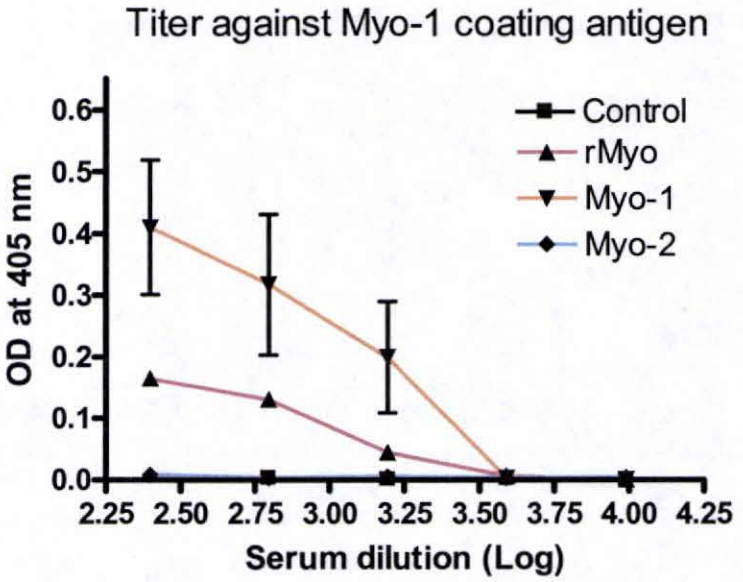

	Serum dilution				
Treatment	**250**	**625**	**1563**	**3906**	**9766**
Control	**-0.001** (0.0027)	**0.003** (0.0031)	**0.001** (0.0029)	**0.002** (0.0030)	**0.001** (0.0030)
rMyo	**0.165** (0.0047)	**0.130** (0.0043)	**0.044** (0.0071)	**0.007** (0.0047)	**0.000** (0.0014)
Myo-1	**0.410** (0.1096)	**0.317** (0.1137)	**0.199** (0.0907)	**0.003** (0.0058)	**0.001** (0.0034)
Myo-2	**0.008** (0.0018)	**0.003** (0.0023)	**0.005** (0.0031)	**0.003** (0.0010)	**0.004** (0.0010)

C) Sera titer curves of immunized female mice using Myo-2-BSA as a coating antigen

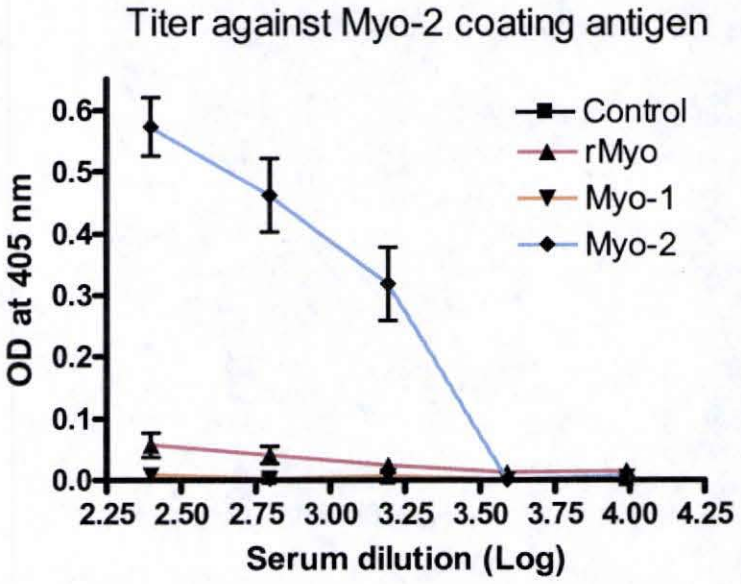

	Serum dilution				
Treatment	**250**	**625**	**1563**	**3906**	**9766**
Control	**-0.001** (0.0008)	**0.003** (0.0024)	**0.003** (0.0020)	**-0.001** (0.0009)	**0.000** (0.0012)
rMyo	**0.057** (0.0199)	**0.041** (0.0139)	**0.024** (0.0093)	**0.012** (0.0035)	**0.015** (0.0018)
Myo-1	**0.008** (0.0012)	**0.002** (0.0036)	**0.006** (0.0020)	**0.001** (0.0011)	**0.005** (0.0015)
Myo-2	**0.573** (0.0475)	**0.462** (0.0592)	**0.318** (0.0601)	**0.001** (0.0033)	**0.006** (0.0013)

APPENDIX 3

Individual serum titers of immunized female mice prior to breeding

Treatment Group	Coating Antigen	Mouse #	Sera dilution				
			250	625	1563	3906	9766
Control	**rupMyo**	112	0.000	0.002	0.003	0.003	0.002
		113	0.006	0.001	-0.001	0.002	-0.001
		114	0.006	0.002	-0.001	0.001	0.002
		115	-0.004	-0.002	0.006	0.002	0.001
		116	0.003	0.001	0.003	-0.002	0.000
		Avg. Titer	**0.002**	**0.001**	**0.002**	**0.001**	**0.001**
	Myo-1	112	-0.001	-0.001	-0.003	-0.002	-0.004
		113	-0.001	0.001	-0.002	0.006	-0.001
		114	0.003	0.007	0.003	0.003	0.002
		115	-0.005	0.003	0.004	0.004	0.004
		116	-0.002	0.005	0.003	0.001	0.003
		Avg. Titer	**-0.001**	**0.003**	**0.001**	**0.002**	**0.001**
	Myo-2	112	0.002	0.003	0.000	-0.003	-0.002
		113	0.000	0.002	0.011	-0.001	0.002
		114	-0.002	0.000	0.000	-0.003	-0.003
		115	-0.003	-0.003	0.002	0.002	0.004
		116	-0.002	0.012	0.003	0.001	0.001
		Avg. Titer	**-0.001**	**0.003**	**0.003**	**-0.001**	**0.000**
rMyo	**rupMyo**	117	0.249	0.147	0.056	0.036	0.008
		118	0.242	0.187	0.059	0.026	0.005
		119	0.192	0.186	0.056	0.030	0.004
		120	0.208	0.259	0.060	0.027	0.004
		121	0.247	0.150	0.082	0.034	0.006
		Avg. Titer	**0.228**	**0.186**	**0.063**	**0.031**	**0.005**
	Myo-1	117	0.156	0.120	0.026	0.011	-0.001
		118	0.165	0.132	0.029	0.019	0.005
		119	0.168	0.129	0.054	0.011	-0.004
		120	0.156	0.125	0.051	-0.009	0.000
		121	0.181	0.145	0.061	0.003	0.000
		Avg. Titer	**0.165**	**0.130**	**0.044**	**0.007**	**0.000**
	Myo-2	117	0.128	0.076	0.044	0.011	0.012
		118	0.024	0.015	0.004	0.003	0.013
		119	0.024	0.017	0.009	0.018	0.020
		120	0.074	0.073	0.049	0.022	0.018
		121	0.038	0.024	0.014	0.006	0.011
		Avg. Titer	**0.057**	**0.041**	**0.024**	**0.012**	**0.015**

(Continued)

Treatment Group	Coating Antigen	Mouse #	Sera dilution 250	625	1563	3906	9766
Myo-1	**rupMyo**	122	0.614	0.402	0.211	0.070	0.015
		123	0.498	0.375	0.220	0.067	0.006
		124	0.519	0.343	0.181	0.056	0.018
		125	0.508	0.298	0.207	0.057	-0.009
		251	0.492	0.295	0.198	0.056	0.002
		Avg. Titer	**0.526**	**0.343**	**0.203**	**0.061**	**0.006**
	Myo-1	122	0.761	0.736	0.542	0.004	0.002
		123	0.327	0.219	0.069	0.002	0.005
		124	0.082	0.049	0.031	-0.014	-0.013
		125	0.419	0.296	0.194	0.023	0.007
		251	0.461	0.288	0.160	0.002	0.004
		Avg. Titer	**0.410**	**0.317**	**0.199**	**0.003**	**0.001**
	Myo-2	122	0.010	-0.002	0.003	0.001	0.006
		123	0.005	-0.008	0.005	0.002	0.006
		124	0.006	0.000	0.001	0.004	0.011
		125	0.011	0.007	0.007	-0.003	0.004
		251	0.007	0.013	0.013	0.000	0.001
		Avg. Titer	**0.008**	**0.002**	**0.006**	**0.001**	**0.005**
Myo-2	**rupMyo**	252	0.385	0.300	0.185	0.047	0.033
		253	0.226	0.219	0.137	0.029	0.013
		254	0.249	0.178	0.107	0.002	-0.003
		255	0.256	0.160	0.085	0.005	0.020
		256	0.396	0.343	0.287	0.047	0.041
		Avg. Titer	**0.302**	**0.240**	**0.160**	**0.026**	**0.021**
	Myo-1	252	0.014	0.006	0.008	0.004	0.006
		253	0.005	0.005	0.003	-0.001	0.003
		254	0.010	0.008	0.014	0.004	0.007
		255	0.008	0.001	0.005	0.002	0.005
		256	0.004	-0.005	-0.005	0.006	0.002
		Avg. Titer	**0.008**	**0.003**	**0.005**	**0.003**	**0.004**
	Myo-2	252	0.457	0.338	0.207	0.010	0.010
		253	0.468	0.368	0.217	0.005	0.009
		254	0.600	0.407	0.282	0.005	0.005
		255	0.650	0.548	0.350	-0.006	0.005
		256	0.692	0.651	0.536	-0.006	0.004
		Avg. Titer	**0.573**	**0.462**	**0.318**	**0.001**	**0.006**

Data are individual sera titers at various dilutions that were corrected to the non-antigen coated control well readings at 405 nm. Titers represent the anti-myostatin antibody levels in the immunized female mice just prior to breeding after receiving 2 or 3 boosters based on the titers.

APPENDIX 4
Weekly individual body weights of female mice during immunization regimen

Treatment	Mouse #	0 wk	1 wk	2 wk	3 wk	4 wk	5 wk	6 wk	7 wk
Control	**112**	20.41	21.05	21.90	23.08	21.92	21.35	22.54	21.40
	113	21.90	21.86	23.90	22.78	22.48	22.83	24.30	23.90
	114	21.28	22.16	22.60	22.92	23.80	22.78	23.71	24.36
	115	21.45	23.06	23.20	25.03	24.90	24.12	25.34	25.10
	116	20.10	22.07	22.60	22.24	21.48	22.33	22.53	22.65
rMyo	**117**	20.64	21.27	22.90	22.66	23.06	24.47	23.00	23.03
	118	21.32	21.83	21.60	21.85	22.04	21.66	21.98	21.65
	119	21.60	21.41	21.90	22.31	22.90	22.80	23.01	25.11
	120	21.35	21.60	21.80	22.06	22.32	23.15	22.10	22.07
	121	20.10	19.84	20.80	22.68	22.71	21.89	21.90	23.25
Myo-1	**122**	19.08	20.28	20.70	19.92	20.48	20.62	20.88	21.70
	123	21.36	21.86	22.90	22.02	22.42	21.81	22.10	22.15
	124	20.70	21.98	21.20	23.04	21.53	22.80	22.18	21.84
	125	22.45	23.04	22.50	23.27	23.30	25.04	23.86	23.87
	251	20.42	20.13	21.50	21.87	22.62	21.82	22.18	22.50
Myo-2	**252**	21.60	23.08	22.30	23.86	25.50	24.22	26.15	24.62
	253	22.76	23.30	24.60	25.97	27.42	25.13	25.74	27.02
	254	19.32	19.79	20.80	22.10	22.02	22.43	21.80	22.36
	255	21.38	22.18	22.30	24.03	22.43	22.60	23.02	24.68
	256	20.08	20.36	21.30	22.04	22.04	21.01	21.10	22.47

Zero Wk denotes the event of primary immunization at which time the female mice were 12-14 wks old. Female mice were given 2-3 boosters 2-3 wks apart based on their titer levels. Body weights were recorded until the mice were bred with male mice.

APPENDIX 5

Summary of sera titers of the 3-day-old neonates

Treatment Group	Coating Antigen	Serum Dilution				
		250	625	1563	3906	9766
Control	**rupMyo**	**0.010** (0.0098)	**0.006** (0.0043)	**0.003** (0.0031)	**0.000** (0.0017)	**-0.001** (0.0021)
	Myo-1	**0.002** (0.0009)	**0.005** (0.0010)	**0.004** (0.0006)	**-0.002** (0.0033)	**-0.001** (0.0019)
	Myo-2	**0.003** (0.0010)	**0.005** (0.0009)	**0.002** (0.0013)	**0.007** (0.0010)	**0.005** (0.0040)
rMyo	**rupMyo**	**0.076** (0.0676)	**0.032** (0.0268)	**0.008** (0.0089)	**0.000** (0.0038)	**-0.010** (0.0003)
	Myo-1	**-0.001** (0.0018)	**0.004** (0.0020)	**0.005** (0.0023)	**-0.002** (0.0013)	**0.000** (0.0013)
	Myo-2	**-0.001** (0.0006)	**0.003** (0.0018)	**0.002** (0.0013)	**-0.004** (0.0045)	**0.000** (0.0007)
Myo-1	**rupMyo**	**0.245** (0.0540)	**0.100** (0.0289)	**0.039** (0.0124)	**0.005** (0.0024)	**0.003** (0.0011)
	Myo-1	**0.049** (0.0120)	**0.036** (0.0083)	**0.024** (0.0070)	**0.000** (0.0009)	**0.007** (0.0013)
	Myo-2	**0.050** (0.0142)	**0.020** (0.0089)	**0.011** (0.0059)	**0.002** (0.0004)	**0.007** (0.0054)
Myo-2	**rupMyo**	**0.053** (0.0357)	**0.023** (0.0153)	**0.009** (0.0058)	**0.007** (0.0018)	**0.002** (0.0005)
	Myo-1	**0.043** (0.0125)	**0.031** (0.0076)	**0.016** (0.0050)	**0.000** (0.0004)	**0.008** (0.0013)
	Myo-2	**0.178** (0.0701)	**0.078** (0.0384)	**0.027** (0.0165)	**-0.005** (0.0045)	**0.004** (0.0008)

The data represent the average OD of duplicates at 405 nm (SEM) corrected to non-antigen-coated control well readings from 1:250 sera dilution. Titers represent the maternally transferred anti-myostatin antibody levels in the offspring from immunized female mice. Three different coating antigens were used: rupMyo, a recombinant unprocessed porcine myostatin, Myo-1-BSA conjugate and Myo-2-BSA conjugate.

APPENDIX 6

A) Sera titer curves of offspring using rupMyo as a coating antigen

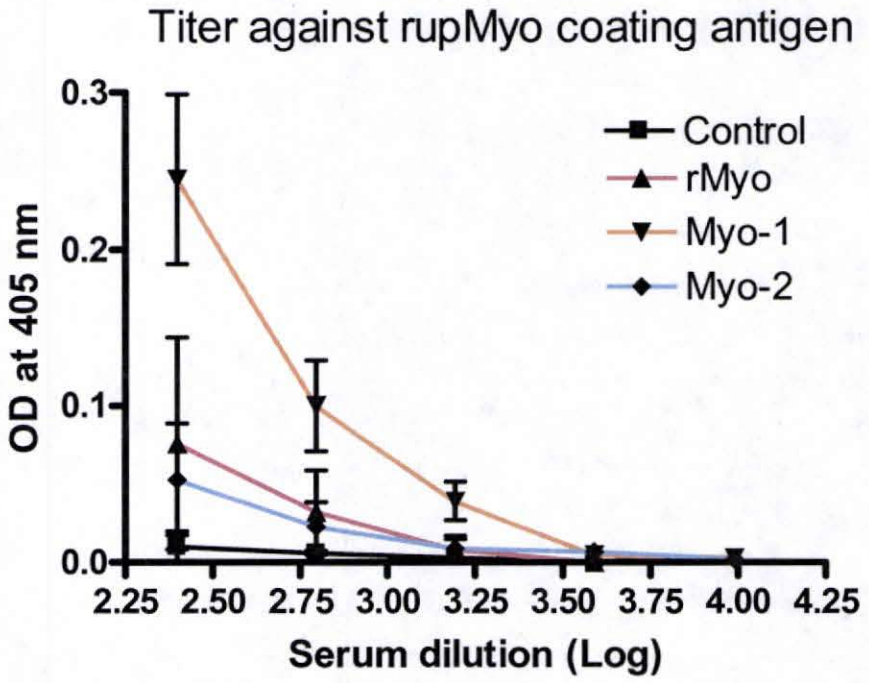

	Serum dilution				
Treatment	**250**	**625**	**1563**	**3906**	**9766**
Control	**0.010** (0.0098)	**0.006** (0.0043)	**0.003** (0.0031)	**0.000** (0.0017)	**-0.001** (0.0021)
rMyo	**0.076** (0.0676)	**0.032** (0.0268)	**0.008** (0.0089)	**0.000** (0.0038)	**-0.010** (0.0003)
Myo-1	**0.245** (0.0540)	**0.100** (0.0289)	**0.039** (0.0124)	**0.005** (0.0024)	**0.003** (0.0011)
Myo-2	**0.053** (0.0357)	**0.023** (0.0153)	**0.009** (0.0058)	**0.007** (0.0018)	**0.002** (0.0005)

B) Sera titer curves of offspring using Myo-1-BSA as a coating antigen

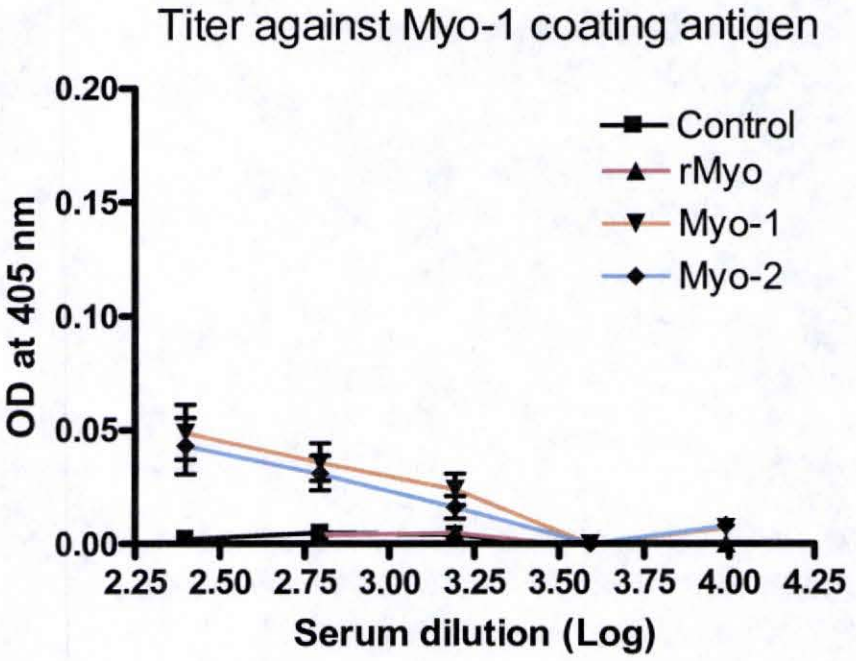

	Serum dilution				
Treatment	**250**	**625**	**1563**	**3906**	**9766**
Control	**0.002** (0.0009)	**0.005** (0.0010)	**0.004** (0.0006)	**-0.002** (0.0033)	**-0.001** (0.0019)
rMyo	**-0.001** (0.0018)	**0.004** (0.0020)	**0.005** (0.0023)	**-0.002** (0.0013)	**0.000** (0.0013)
Myo-1	**0.049** (0.0120)	**0.036** (0.0083)	**0.024** (0.0070)	**0.000** (0.0009)	**0.007** (0.0013)
Myo-2	**0.043** (0.0125)	**0.031** (0.0076)	**0.016** (0.0050)	**0.000** (0.0004)	**0.008** (0.0013)

C) Sera titer curves of offspring using Myo-2-BSA as a coating antigen

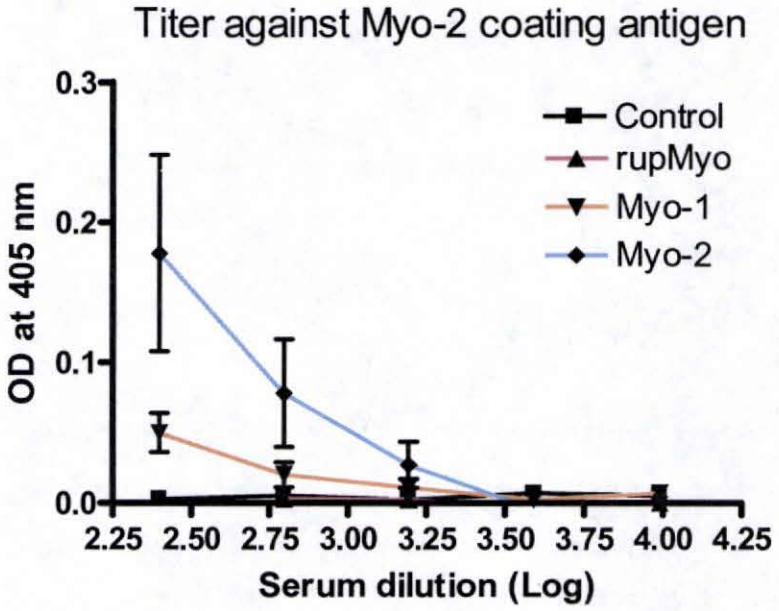

	Serum dilution				
Treatment	**250**	**625**	**1563**	**3906**	**9766**
Control	**0.003** (0.0010)	**0.005** (0.0009)	**0.002** (0.0013)	**0.007** (0.0010)	**0.005** (0.0040)
rMyo	**-0.001** (0.0006)	**0.003** (0.0018)	**0.002** (0.0013)	**-0.004** (0.0045)	**0.000** (0.0007)
Myo-1	**0.050** (0.0142)	**0.020** (0.0089)	**0.011** (0.0059)	**0.002** (0.0004)	**0.007** (0.0054)
Myo-2	**0.178** (0.0701)	**0.078** (0.0384)	**0.027** (0.0165)	**-0.005** (0.0045)	**0.004** (0.0008)

APPENDIX 7

Individual serum titers of the 3-day-old neonates from immunized female mice

Treatment Group	Coating Antigen	Dam #	Serum Dilution				
			250	625	1563	3906	9766
Control	**rupMyo**	112	-0.005	0.006	0.008	0.001	-0.008
		113	-0.001	0.001	0.003	0.005	-0.003
		114	0.048	0.021	0.011	-0.004	0.006
		115	0.005	-0.005	-0.007	-0.004	-0.001
		116	0.001	0.010	-0.001	0.002	0.000
		Avg. Titer	**0.010**	**0.006**	**0.003**	**0.000**	**-0.001**
	Myo-1	112	-0.001	0.002	0.005	-0.012	-0.001
		113	0.002	0.007	0.004	-0.005	0.000
		114	0.005	0.007	0.005	0.006	0.005
		115	0.003	0.004	0.004	0.005	-0.005
		116	0.002	0.008	0.001	-0.005	-0.006
		Avg. Titer	**0.002**	**0.005**	**0.004**	**-0.002**	**-0.001**
	Myo-2	112	0.002	0.003	0.003	0.007	-0.003
		113	0.003	0.003	0.001	0.008	-0.004
		114	0.000	0.008	0.003	0.008	0.002
		115	0.006	0.005	0.005	0.004	0.010
		116	0.003	0.006	-0.003	0.010	0.018
		Avg. Titer	**0.003**	**0.005**	**0.002**	**0.007**	**0.005**
rMyo	**rupMyo**	117	0.017	0.010	-0.003	0.005	-0.009
		118	0.211	0.085	0.026	0.003	-0.010
		119	0.000	0.001	0.002	-0.008	-0.011
		Avg. Titer	**0.076**	**0.032**	**0.008**	**0.000**	**-0.010**
	Myo-1	117	0.002	0.004	0.009	0.001	0.003
		118	-0.005	0.008	0.005	-0.002	-0.002
		119	-0.001	0.001	0.001	-0.004	-0.001
		Avg. Titer	**-0.001**	**0.004**	**0.005**	**-0.002**	**0.000**
	Myo-2	117	-0.002	0.005	0.004	-0.013	-0.001
		118	0.001	0.005	0.001	0.002	0.001
		119	-0.001	-0.001	0.000	-0.001	0.001
		Avg. Titer	**-0.001**	**0.003**	**0.002**	**-0.004**	**0.000**

(Continued)

Treatment Group	Coating Antigen	Dam #	Serum Dilution				
			250	625	1563	3906	9766
Iyo-1	**rupMyo**	122	0.246	0.124	0.069	0.002	0.005
		123	0.397	0.160	0.057	0.005	0.005
		124	0.154	0.058	0.020	0.003	0.002
		125	0.184	0.061	0.010	0.012	0.001
		Avg. Titer	**0.245**	**0.100**	**0.039**	**0.005**	**0.003**
	Myo-1	122	0.049	0.043	0.039	0.002	0.010
		123	0.066	0.041	0.032	0.001	0.003
		124	0.015	0.015	0.004	-0.003	0.008
		125	0.067	0.046	0.020	0.001	0.007
		Avg. Titer	**0.049**	**0.036**	**0.024**	**0.000**	**0.007**
	Myo-2	122	0.042	0.029	0.030	0.000	0.004
		123	0.060	0.022	0.016	0.002	0.001
		124	0.015	-0.003	-0.008	0.002	0.003
		125	0.082	0.032	0.004	0.004	0.021
		Avg. Titer	**0.050**	**0.020**	**0.011**	**0.002**	**0.007**
Iyo-2	**rupMyo**	252	0.039	0.021	0.006	0.001	0.005
		253	0.158	0.059	0.023	0.012	0.000
		254	0.006	0.011	0.006	0.005	0.003
		255	0.011	0.002	0.001	0.010	0.001
		Avg. Titer	**0.053**	**0.023**	**0.009**	**0.007**	**0.002**
	Myo-1	252	0.017	0.014	0.005	0.001	0.007
		253	0.074	0.055	0.031	0.001	0.009
		254	0.030	0.031	0.017	-0.001	0.006
		255	0.050	0.026	0.011	0.001	0.011
		Avg. Titer	**0.043**	**0.031**	**0.016**	**0.000**	**0.008**
	Myo-2	252	0.239	0.114	0.039	0.000	0.004
		253	0.348	0.169	0.068	0.002	0.007
		254	0.063	0.015	-0.005	-0.018	0.003
		255	0.063	0.014	0.007	-0.004	0.004
		Avg. Titer	**0.178**	**0.078**	**0.027**	**-0.005**	**0.004**

One, 3-day old neonate from each litter was sacrificed for serum titer evaluation. The data represent the average OD of duplicates at 405 nm ± SEM corrected to non-antigen coated control well readings from 1:250 sera dilution. Titers represent the maternally transferred anti-myostatin antibody levels in the offspring from immunized female mice.

APPENDIX 8

Pre-weaning body weights of the offspring (1-3 Wks)

Treatment	Dam #	Litter size	Male	Female	1 Wk	2 Wk	3 Wk
Control	**112**	8	5	3	4.03	7.43	8.80
	113	9	4	5	3.70	7.10	9.43
	114	7	5	2	3.80	7.03	10.01
	115	8	5	3	4.05	7.13	11.28
	116	8	5	3	4.15	6.76	8.03
rMyo	**117**	5	3	1	3.92	7.00	8.76
	118	5	4	1	4.64	7.43	10.18
	121	9	5	4	3.88	6.23	8.45
Myo-1	**122**	5	1	4	4.77	8.06	11.22
	124	7	2	5	3.94	7.38	10.11
	125	8	3	5	4.99	7.69	10.04
	251	8	0	8	4.51	7.13	9.50
Myo-2	**252**	9	6	3	4.20	7.10	9.64
	253	6	3	3	4.92	7.85	10.45
	254	8	3	5	4.37	7.88	9.91
	255	7	2	5	3.30	7.30	9.28

The littermates from immunized female mice were weighed collectively up to 3 weeks and weaned at 3rd week based on sex. The data are average body weights of whole litter (including males and females).

APPENDIX 9

Post-weaning body weights of the offspring (4-8 Wks)

Treatment group	Dam #	Sex	No. of mice	4 wk	5 wk	6 wk	7 wk	8 wk
Control	**112**	1	5	16.16	20.26	21.36	26.69	23.05
		2	3	12.46	13.22	14.81	15.43	15.28
	113	1	4	15.86	20.65	22.42	23.74	24.70
		2	5	12.11	14.03	15.11	16.19	16.56
	114	1	5	18.61	20.54	21.57	23.14	23.41
		2	2	15.53	16.81	18.96	19.75	18.93
	115	1	5	18.56	21.06	22.86	24.53	24.25
		2	3	16.45	17.72	18.45	19.87	19.12
	116	1	5	12.99	18.80	20.66	22.62	22.68
		2	3	12.74	16.33	17.11	17.87	17.66
rMyo	**117**	1	3	15.17	20.29	21.07	19.07	21.51
		2	1	15.40	19.04	19.30	19.32	18.92
	118	1	4	15.76	19.76	21.91	24.00	24.41
		2	1	15.30	18.16	18.56	20.50	19.96
	121	1	5	14.68	19.59	21.10	21.60	22.17
		2	4	11.77	14.20	15.78	16.78	17.44
Myo-1	**122**	1	1	16.60	19.35	20.26	22.50	22.60
		2	4	14.11	16.80	16.93	17.36	18.40
	124	1	2	14.80	19.71	21.23	23.70	23.22
		2	5	12.98	15.86	15.48	16.64	16.91
	125	1	3	16.76	19.93	21.46	24.03	24.66
		2	5	13.72	16.49	16.73	18.16	18.57
	251	2	8	14.64	16.44	16.64	17.57	17.55
Myo-2	**252**	1	6	14.05	19.82	21.94	23.50	24.95
		2	3	12.94	17.10	17.56	18.88	19.65
	253	1	3	14.49	19.27	21.36	22.24	23.50
		2	3	14.36	15.93	17.40	17.90	18.55
	254	1	3	14.77	19.44	21.80	23.57	23.69
		2	5	13.21	16.32	17.70	18.76	18.31
	255	1	2	18.02	20.52	21.35	22.26	23.63
		2	5	14.52	16.02	16.44	17.53	18.52

Data are the average body weights of male, female littermates separately; 1, male, 2, female. Two mice in rMyo group, one each in Myo-1 and Myo-2 were unable to produce offspring even after repeated attempts.

APPENDIX 10
SDS-PAGE analysis of affinity-purified antibodies from immune sera

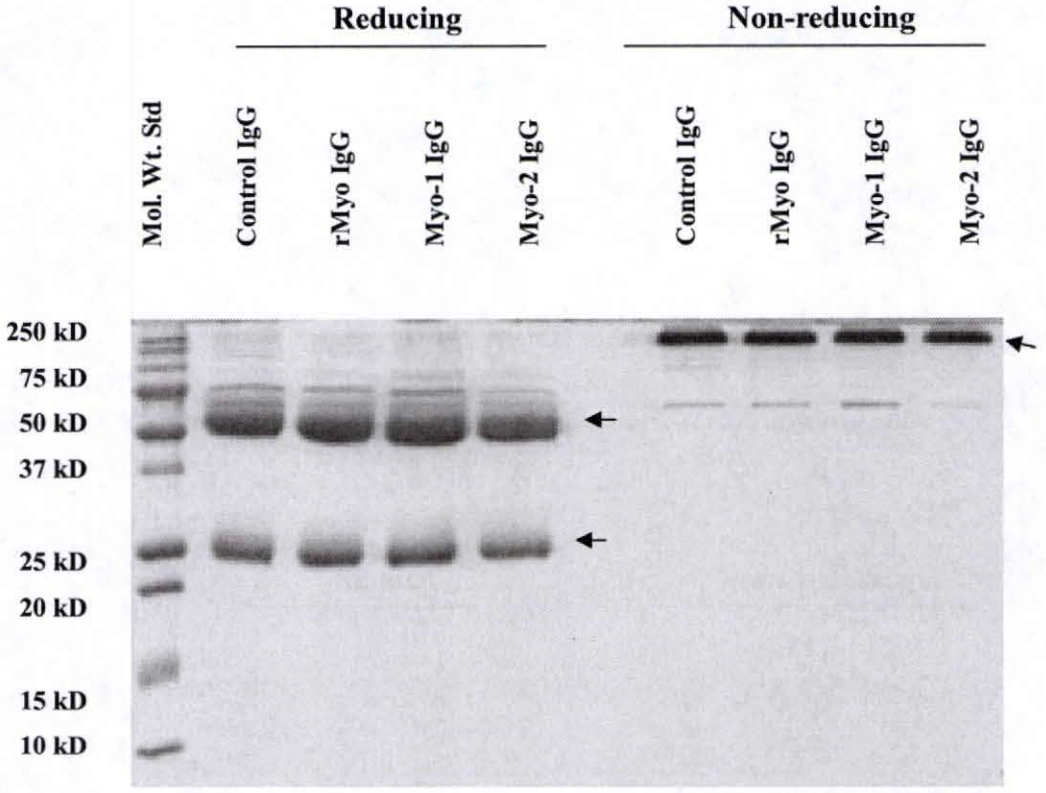

Affinity-purified antibodies (4 µg) were subjected to 15 % SDS-PAGE in either reducing (2-Mercaptoethanol) or non-reducing conditions and visualized using Coomassie blue stain. Arrows in reducing condition indicate IgG heavy chain (50 kD) and light chains (25 kD), respectively. Arrow in non-reducing condition indicates the native form of immunoglobulins (150 kD).

APPENDIX 11

Effect of myostatin on pGL3 $(CAGA)_{12}$ Luc-luciferase reporter system

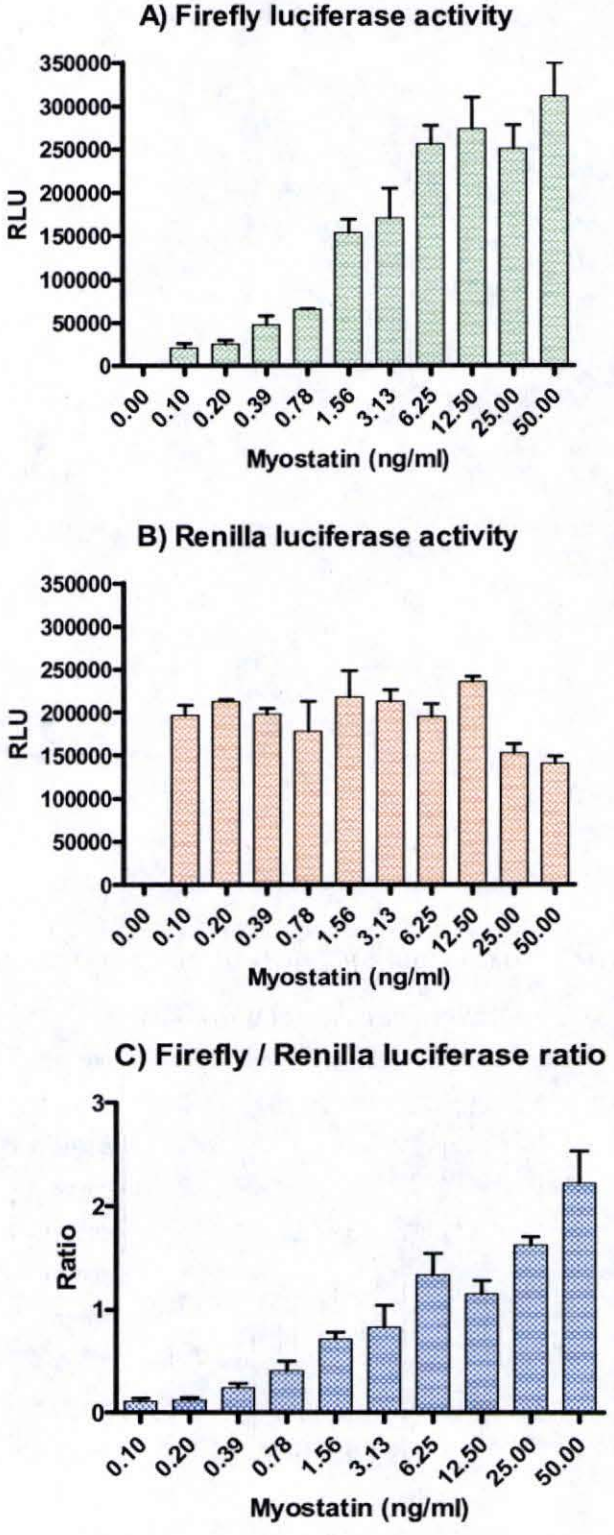

	Firefly luciferase activity			Renilla luciferase activity			Firefly / Renilla ratio		
MSTN (ng/ml)	**Rep 1**	**Rep 2**	**Rep 3**	**Rep 1**	**Rep 2**	**Rep 3**	**Rep 1**	**Rep 2**	**Rep 3**
No transfection	72	68	66	78	95	110	0.92	0.72	0.60
0.1	17593	13425	31795	219439	176491	192149	1.72	1.96	1.74
0.2	31262	29107	16303	209272	214678	215443	2.05	1.81	2.82
0.39	37789	67772	38689	186120	209785	198081	1.62	1.50	1.76
0.78	64211	65342	66844	233853	112741	186863	1.00	1.40	1.07
1.56	169362	121781	169835	202738	174388	277143	1.03	1.73	1.26
3.13	219048	187770	106192	189227	211581	237333	1.16	0.89	0.45
6.25	215247	287565	265688	208176	166313	210974	0.84	0.70	0.61
12.5	228109	345645	248761	229103	246778	232339	0.27	0.58	0.36
25	245319	205890	301204	151403	137282	170661	0.20	0.32	0.20
50	321527	242707	371551	156568	134176	131845	0.15	0.14	0.08
100	755072	453962	524050	439617	231646	301440	0.08	0.08	0.17

A204 cells were seeded (40,000 cells/ml) on a 96-well culture plate and grown on DMEM with 10% fetal calf serum, antibiotic and antimycotic. After 36 hours, a mixture containing 0.2 μg of pGL3 $(CAGA)_{12}$ Luc-luciferase plasmid, 0.05 μg of pRL-TK- Renilla luciferase plasmid and 0.5 μl of Lipofectamine in antibiotic-free DMEM containing 10% FCS . After 24 hours of transfection, the cells were serum starved for 9 hours. After serum starvation, myostatin in serial dilutions was added to each well in triplicates followed by incubation for 6-8 hours. Luciferase activity was measured by Veritas microplate luminometer (Turner Biosystems Inc, CA) using two different substrates for firefly and renilla luciferase enzymes. Figures A, B, and C represent the effect of myostatin on pGL3 $(CAGA)_{12}$ Luc-luciferase plasmid, pRL-TK-Renilla luciferase plasmid and luc-luciferase to renilla luciferase ratio, respectively.

APPENDIX 12

Effects of affinity-purified antibody on myostatin's activity in pGL3 $(CAGA)_{12}$ Luc-luciferase reporter system.

IgG (ng/ml)	Control IgG				rMyo IgG				Myo-1 IgG				Myo-2 IgG			
	1	2	3	4	1	2	3	4	1	2	3	4	1	2	3	4
7	1.02	0.89	1.25	1.36	1.42	1.29	1.05	1.40	1.04	1.26	1.18	0.98	1.20	1.44	1.66	1.77
14	1.06	0.96	0.91	0.90	0.86	0.79	1.09	1.80	0.96	1.40	1.39	1.21	1.45	1.76	1.80	2.27
28	0.99	1.06	0.76	1.05	1.34	1.13	0.85	1.92	0.90	1.32	0.97	1.07	1.21	1.64	1.53	2.33
56	1.00	0.89	1.20	0.82	1.13	0.88	1.11	2.19	1.47	1.43	1.56	0.85	1.54	1.73	1.46	2.10
113	1.01	1.57	1.04	1.16	1.29	1.13	1.16	2.02	0.87	1.16	1.25	0.93		1.34	1.63	1.73
225	0.98	1.06		1.10	1.22	0.82	1.21	1.75	1.16	1.44	1.41	1.03	1.45	1.89	1.40	1.63
450	1.08	0.92	1.40	1.19	1.31	0.90	1.23	1.65	0.93	1.05	0.93	1.09	1.47	1.16	1.46	1.15
No Mstn	0.03		0.04	0.05	0.04	0.03	0.03	0.04	0.05	0.04	0.05	0.04	0.04	0.04	0.04	0.08
Mstn only	0.96	0.70	0.87	1.04	1.08	0.93	1.16	1.23	1.80	1.11	1.39	1.51	1.99	1.94	1.79	1.41
Mstn + Prod	0.06	0.03	0.02	0.06	0.05	0.04	0.07		0.05	0.05	0.09	0.08	0.07	0.10	0.06	0.09

A204 cells were seeded (40,000 cells/ml) on a 96-well culture plate and grown on DMEM with 10% fetal calf serum, antibiotic and antimycotic. After 36 hours, a mixture containing 0.2 µg of pGL3 $(CAGA)_{12}$ Luc-luciferase plasmid, 0.05 µg of pRL-TK- Renilla luciferase plasmid and 0.5 µl of Lipofectamine 2000 in antibiotic-free DMEM containing 10% FCS . After 24 hours of transfection, the cells were serum starved for 9 hours. After serum starvation, myostatin (5 ng/ml) and various dilutions of the affinity-purified IgGs were added to each well in quadruplets followed by incubation for 6-8 hours. Luciferase activity was measured by Veritas microplate luminometer (Turner Biosystems Inc, CA) using two different substrates for firefly and renilla luciferase enzymes. Figures A, B, C and D bar diagrams represent the ratios of firefly luciferase to renilla luciferase in affinity-purified IgG treated wells from control, rMyo, Myo-1 and Myo-2, respectively. Positive controls were maintained on 5 ng/ml myostatin and 30 ng/ml prodomain while negative controls were on 5 ng/ml myostatin, without prodomain.

APPENDIX 13.

Effects affinity-purified antibody (high conc.) on myostatin's activity on pGL3 $(CAGA)_{12}$ Luc-luciferase reporter system

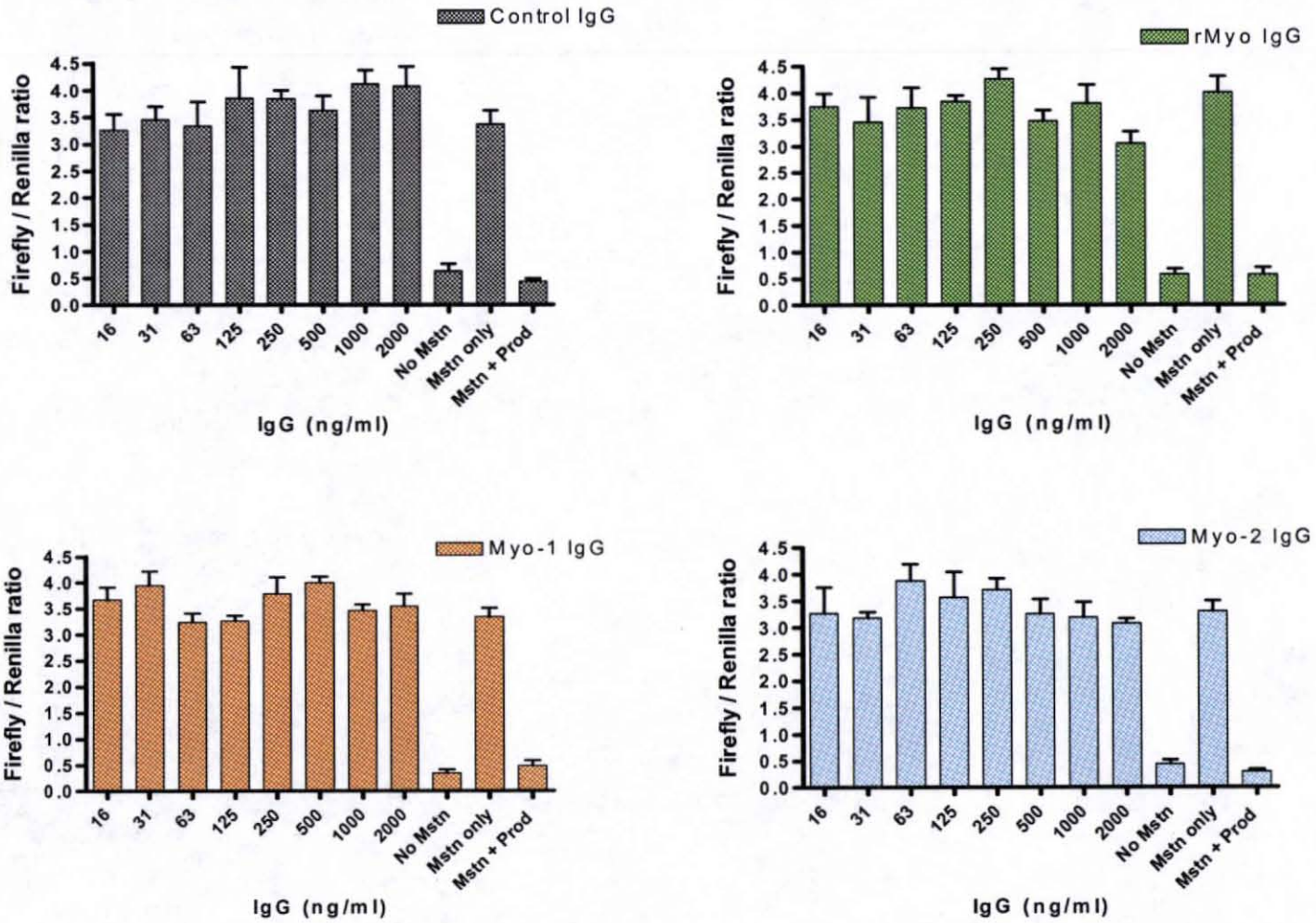

IgG (ng/ml)	Control IgG				rMyo IgG				Myo-1 IgG				Myo-2 IgG			
Replicates	1	2	3	4	1	2	3	4	1	2	3	4	1	2	3	4
16	3.30	4.08	2.69	2.97	3.70	4.20	3.07	3.99	3.39	3.65	3.29	4.36	3.10	4.36	3.57	2.03
31	3.68	3.95	3.39	2.82	3.22	2.59	4.79	3.21	3.43	4.10	4.64	3.63	3.05	3.32	2.95	3.40
63	2.62	3.72	2.61	4.43	3.33	4.66	3.98	2.89	2.97	3.54	3.22		3.59	4.81	3.46	3.63
125	4.17	4.43	2.17	4.68	3.96	4.07	3.55	3.77	3.39	3.35	3.37	2.97	3.74	2.17	3.97	4.37
250	3.50	3.69	4.00	4.18	4.43	3.91	3.99	4.72	4.41	3.74	4.08	2.91	4.08	3.17	3.98	3.62
500	3.17	4.03	3.12	4.16	3.06	4.01	3.29	3.53	3.70	4.23	3.99	4.09	2.49	3.23	3.84	3.45
1000	3.65	4.54	4.56	3.74	3.46	3.01	4.40	4.37	3.54	3.62	3.58	3.12	4.05	2.87	2.89	2.93
2000	3.37	5.08	3.86	4.02	2.98	3.51	3.24	2.49	4.17	3.20	3.67	3.15	2.97	3.26	2.88	3.18
No Mstn	0.43	0.38	0.79	0.93	0.62	0.66	0.75	0.31	0.24	0.34	0.22	0.57	0.55	0.55	0.44	0.21
Mstn only	4.13	3.04	3.16	3.13	4.08	4.47	4.36	3.11	2.99	3.84	3.22	3.32	3.28	3.30	3.05	3.78
Mstn + Prod	0.27	0.48	0.47	0.53	0.39	0.98	0.45	0.47	0.23	0.47	0.45	0.77	0.25	0.37	0.18	0.38

A204 cells were seeded (40,000 cells/ml) on a 96-well culture plate and grown on DMEM with 10% fetal calf serum, antibiotic and antimycotic. After 36 hours, a mixture containing 0.2 µg of pGL3 $(CAGA)_{12}$ Luc-luciferase plasmid, 0.05 µg of pRL-TK-Renilla luciferase plasmid and 0.5 µl of lipofectamine 2000 in antibiotic-free DMEM containing 10% FCS . After 24 hours of transfection, the cells were serum starved for 9 hours. After serum starvation, myostatin (5 ng/ml) and various dilutions of the affinity-purified IgGs were added to each well in quadruplets followed by incubation for 6-8 hours. Luciferase activity was measured by Veritas microplate luminometer (Turner Biosystems Inc, CA) using two different substrates for firefly and renilla luciferase enzymes. Figures A, B, C and D bar diagrams represent the ratios of firefly luciferase to renilla luciferase in affinity-purified IgG treated wells from control, rMyo, Myo-1 and Myo-2, respectively. Positive controls were maintained on 5 ng/ml myostatin and 30 ng/ml prodomain while negative controls were on 5 ng/ml myostatin, without prodomain.

APPENDIX 14. Individual body weights and carcass characteristics of offspring at 8 wks of age

Treatment	Dam #	Sex	Total Wt.	Carcass wt	Carcass %	Gas (Avg)	Gas%	Triceps (Avg)	Tri %	Visceral Fat	V.Fat	Brown fat	Brown fat %
0	112	1	22.07	7.93	35.93	0.1115	0.51	0.0614	0.28	0.3026	1.37	0.1230	0.56
0	112	1	21.53	7.99	37.11	0.1169	0.54	0.0706	0.33	0.1346	0.63	0.1009	0.47
0	112	1	24.29	8.89	36.60	0.1320	0.54	0.0826	0.34	0.2628	1.08	0.1919	0.79
0	112	1	24.48	9.23	37.70	0.1371	0.56	0.0801	0.33	0.4130	1.69	0.1433	0.59
0	112	1	22.88	8.80	38.46	0.1321	0.58	0.0834	0.36	0.1360	0.59	0.0974	0.43
0	112	2	15.74	5.51	35.01	0.0632	0.40	0.0521	0.33	0.0160	0.10	0.0491	0.31
0	112	2	15.26	5.37	35.19	0.0660	0.43	0.0441	0.29	0.0350	0.23	0.0852	0.56
0	112	2	14.84	4.99	33.63	0.0623	0.42	0.0449	0.30	0.0570	0.38	0.0840	0.57
0	113	1	24.50	8.73	35.63	0.1390	0.57	0.0936	0.38	0.2943	1.20	0.1343	0.55
0	113	1	26.30	9.86	37.49	0.1552	0.59	0.0978	0.37	0.2790	1.06	0.1606	0.61
0	113	1	22.80	8.96	39.30	0.1296	0.57	0.0829	0.36	0.1080	0.47	0.0850	0.37
0	113	1	25.20	9.57	37.98	0.1400	0.56	0.0955	0.38	0.1910	0.76	0.1300	0.52
0	113	2	17.43	5.90	33.85	0.0834	0.48	0.0505	0.29	0.0640	0.37	0.1169	0.67
0	113	2	16.46	5.80	35.24	0.0782	0.48	0.0579	0.35	0.0350	0.21	0.0700	0.43
0	113	2	16.50	5.61	34.00	0.0771	0.47	0.0577	0.35	0.0606	0.37	0.1075	0.65
0	113	2	17.55	6.38	36.35	0.0855	0.49	0.0626	0.36	0.0502	0.29	0.0757	0.43
0	113	2	14.88	5.11	34.34	0.0740	0.50	0.0465	0.31	0.0313	0.21	0.0742	0.50
0	114	1	25.76	9.30	36.10	0.1434	0.56	0.1015	0.39	0.2722	1.06	0.1568	0.61
0	114	1	24.24	9.44	38.94	0.1415	0.58	0.0895	0.37	0.1583	0.65	0.1420	0.59
0	114	1	21.36	7.51	35.16	0.1098	0.51	0.0791	0.37	0.1133	0.53	0.1210	0.57
0	114	1	24.62	9.17	37.25	0.1300	0.53	0.0853	0.35	0.3462	1.41	0.1418	0.58
0	114	1	21.08	7.56	35.86	0.1150	0.55	0.0764	0.36	0.2829	1.34	0.1407	0.67
0	114	2	20.16	6.95	34.47	0.1047	0.52	0.0627	0.31	0.0924	0.46	0.1408	0.70
0	114	2	17.70	6.42	36.27	0.1005	0.57	0.0623	0.35	0.0973	0.55	0.1050	0.59
0	115	1	24.67	9.44	38.27	0.1597	0.65	0.0989	0.40	0.2727	1.11	0.0969	0.39
0	115	1	20.32	7.37	36.27	0.1155	0.57	0.0732	0.36	0.1090	0.54	0.1330	0.65
0	115	1	23.76	8.97	37.75	0.1385	0.58	0.0945	0.40	0.2080	0.88	0.1196	0.50
0	115	1	26.59	9.94	37.38	0.1502	0.56	0.0859	0.32	0.1440	0.54	0.1210	0.46
0	115	1	25.90	10.05	38.80	0.1512	0.58	0.0988	0.38	0.2110	0.81	0.1223	0.47
0	115	2	20.31	6.64	32.69	0.1145	0.56	0.0677	0.33	0.0506	0.25	0.1316	0.65
0	115	2	18.14	6.53	36.00	0.0920	0.51	0.0653	0.36	0.0833	0.46	0.0800	0.44

(Continued)

Treatment	Dam #	Sex	Total Wt.	Carcass wt	Carcass %	Gas (Avg)	Gas%	Triceps (Avg)	Tri %	Visceral Fat	V.Fat	Brown fat	Brown fat %
0	116	1	25.41	9.69	38.13	0.1327	0.52	0.0988	0.39	0.2570	1.01	0.1230	0.48
0	116	1	23.97	9.75	40.68	0.1400	0.58	0.0938	0.39	0.1812	0.76	0.1160	0.48
0	116	1	21.08	7.86	37.29	0.1198	0.57	0.0842	0.40	0.2718	1.29	0.1340	0.64
0	116	1	21.44	8.17	38.11	0.1112	0.52	0.0641	0.30	0.1490	0.69	0.0964	0.45
0	116	1	21.48	8.35	38.87	0.1324	0.62	0.0745	0.35	0.1550	0.72	0.0956	0.45
0	116	2	17.89	6.55	36.61	0.1081	0.60	0.0654	0.37	0.0815	0.46	0.0704	0.39
0	116	2	18.56	6.62	35.67	0.0985	0.53	0.0709	0.38	0.0805	0.43	0.0694	0.37
0	116	2	16.52	6.15	37.23	0.0867	0.52	0.0552	0.33	0.0687	0.42	0.0783	0.47
1	117	1	21.83	8.45	38.71	0.1130	0.52	0.0619	0.28	0.1502	0.69	0.1218	0.56
1	117	1	23.31	9.36	40.15	0.1366	0.59	0.0810	0.35	0.1862	0.80	0.1041	0.45
1	117	1	19.39	7.48	38.58	0.1183	0.61	0.0686	0.35	0.1502	0.77	0.0990	0.51
1	117	2	18.92	6.83	36.10	0.0736	0.39	0.0557	0.29	0.1190	0.63	0.1420	0.75
1	118	1	26.20	9.56	36.49	0.1452	0.55	0.1020	0.39	0.2510	0.96	0.1620	0.62
1	118	1	24.30	9.12	37.53	0.1505	0.62	0.0877	0.36	0.2260	0.93	0.1063	0.44
1	118	1	22.80	8.49	37.24	0.1392	0.61	0.0819	0.36	0.1715	0.75	0.0773	0.34
1	118	1	24.35	8.85	36.34	0.1357	0.56	0.0835	0.34	0.1450	0.60	0.1542	0.63
1	118	2	19.96	7.25	36.32	0.1132	0.57	0.0684	0.34	0.1156	0.58	0.0968	0.48
1	121	1	23.34	8.55	36.63	0.1229	0.53	0.0867	0.37	0.0812	0.35	0.1020	0.44
1	121	1	21.02	7.77	36.96	0.1115	0.53	0.0869	0.41	0.1917	0.91	0.0817	0.39
1	121	1	22.16	7.78	35.11	0.1194	0.54	0.0801	0.36	0.1770	0.80	0.1590	0.72
1	121	2	17.03	5.84	34.29	0.0823	0.48	0.0617	0.36	0.0563	0.33	0.0603	0.35
1	121	2	17.78	6.26	35.21	0.0914	0.51	0.0629	0.35	0.1710	0.96	0.1240	0.70
1	121	2	16.18	5.65	34.92	0.0781	0.48	0.0488	0.30	0.1100	0.68	0.0565	0.35
1	121	2	18.78	6.03	32.11	0.0816	0.43	0.0563	0.30	0.1792	0.95	0.0816	0.43
2	122	1	22.60	8.43	37.30	0.1343	0.59	0.0800	0.35	0.2001	0.89	0.1052	0.47
2	122	2	19.73	6.78	34.36	0.0843	0.43	0.0636	0.32	0.0390	0.20	0.0736	0.37
2	122	2	17.20	6.32	36.74	0.0979	0.57	0.0631	0.37	0.0878	0.51	0.0893	0.52
2	122	2	17.90	6.32	35.31	0.0918	0.51	0.0611	0.34	0.0698	0.39	0.0902	0.50
2	122	2	18.77	6.57	35.00	0.0994	0.53	0.0558	0.30	0.1150	0.61	0.0980	0.52
2	124	1	23.35	8.76	37.52	0.1430	0.61	0.0992	0.42	0.1430	0.61	0.0805	0.34
2	124	1	23.08	8.60	37.26	0.1378	0.60	0.0825	0.36	0.1387	0.60	0.1120	0.49
2	124	2	17.90	6.38	35.64	0.0827	0.46	0.0597	0.33	0.0830	0.46	0.0664	0.37

(Continued)

Treatment	Dam #	Sex	Total Wt.	Carcass wt	Carcass %	Gas (Avg)	Gas%	Triceps (Avg)	Tri %	Visceral Fat	V.Fat	Brown fat	Brown fat %
2	124	2	17.02	6.17	36.25	0.0887	0.52	0.0576	0.34	0.0967	0.57	0.1166	0.69
2	124	2	17.08	6.34	37.12	0.0827	0.48	0.0612	0.36	0.1204	0.70	0.0614	0.36
2	124	2	17.28	5.94	34.38	0.0898	0.52	0.0627	0.36	0.1824	1.06	0.0706	0.41
2	125	1	25.02	9.36	37.41	0.1392	0.56	0.0811	0.32	0.2690	1.08	0.2070	0.83
2	125	1	24.30	9.81	40.37	0.1430	0.59	0.0907	0.37	0.1660	0.68	0.1044	0.43
2	125	2	17.81	6.30	35.37	0.0896	0.50	0.0619	0.35	0.0989	0.56	0.0850	0.48
2	125	2	18.60	6.59	35.43	0.0954	0.51	0.0616	0.33	0.1118	0.60	0.1117	0.60
2	125	2	18.96	7.08	37.34	0.1039	0.55	0.0660	0.35	0.0650	0.34	0.0687	0.36
2	125	2	17.08	6.44	37.70	0.0939	0.55	0.0591	0.35	0.0906	0.53	0.0794	0.46
2	125	2	20.38	7.55	37.05	0.1022	0.50	0.0735	0.36	0.1570	0.77	0.0791	0.39
2	251	2	16.67	6.11	36.65	0.0921	0.55	0.0534	0.32	0.1140	0.68	0.0749	0.45
2	251	2	19.64	7.01	35.69	0.0998	0.51	0.0597	0.30	0.1457	0.74	0.1053	0.54
2	251	2	16.67	5.71	34.25	0.0781	0.47	0.0561	0.34	0.1115	0.67	0.0820	0.49
2	251	2	16.76	6.12	36.52	0.0940	0.56	0.0508	0.30	0.2100	1.25	0.1230	0.73
2	251	2	18.01	5.56	30.87	0.0841	0.47	0.0495	0.27	0.0824	0.46	0.0810	0.45
2	251	2	17.78	6.32	35.55	0.0926	0.52	0.0581	0.33	0.0847	0.48	0.0742	0.42
2	251	2	17.32	6.44	37.18	0.0830	0.48	0.0592	0.34	0.0667	0.39	0.1490	0.86
2	251	2	17.53	6.22	35.48	0.0812	0.46	0.0541	0.31	0.1045	0.60	0.0697	0.40
3	252	1	23.72	9.61	40.51	0.1501	0.63	0.1013	0.43	0.1353	0.57	0.0888	0.37
3	252	1	26.43	9.54	36.10	0.1399	0.53	0.0950	0.36	0.3813	1.44	0.2049	0.78
3	252	1	23.61	8.92	37.78	0.1436	0.61	0.0882	0.37	0.3400	1.44	0.1561	0.66
3	252	1	25.90	9.95	38.42	0.1405	0.54	0.1097	0.42	0.2970	1.15	0.1234	0.48
3	252	1	25.96	9.19	35.40	0.1436	0.55	0.1056	0.41	0.2727	1.05	0.0976	0.38
3	252	1	24.05	8.55	35.55	0.1396	0.58	0.0931	0.39	0.3083	1.28	0.1707	0.71
3	252	2	17.62	6.19	35.13	0.0944	0.54	0.0628	0.36	0.0539	0.31	0.1026	0.58
3	252	2	20.43	7.38	36.12	0.1041	0.51	0.0696	0.34	0.1270	0.62	0.0750	0.37
3	252	2	20.89	8.10	38.77	0.1102	0.53	0.0818	0.39	0.0642	0.31	0.0892	0.43
3	253	1	23.90	8.99	37.62	0.1465	0.61	0.0988	0.41	0.2537	1.06	0.1578	0.66
3	253	1	23.30	8.88	38.11	0.1432	0.61	0.0854	0.37	0.1095	0.47	0.0971	0.42
3	253	1	23.31	8.12	34.83	0.1237	0.53	0.0828	0.35	0.2406	1.03	0.1528	0.66
3	253	2	17.52	6.01	34.30	0.0898	0.51	0.0554	0.32	0.1502	0.86	0.0960	0.55
3	253	2	18.26	6.42	35.16	0.1003	0.55	0.0650	0.36	0.0651	0.36	0.0810	0.44

(Continued)

Treatment	Dam #	Sex	Total Wt.	Carcass wt	Carcass %	Gas (Avg)	Gas%	Triceps (Avg)	Tri %	Visceral Fat	V.Fat	Brown fat	Brown fat %
3	254	1	24.18	8.67	35.86	0.1323	0.55	0.0889	0.37	0.2353	0.97	0.1213	0.50
3	254	1	22.85	9.02	39.47	0.1543	0.68	0.0966	0.42	0.1360	0.60	0.0750	0.33
3	254	1	24.03	9.28	38.62	0.1546	0.64	0.0950	0.40	0.2735	1.14	0.1821	0.76
3	254	2	19.48	6.88	35.32	0.1059	0.54	0.0638	0.33	0.1496	0.77	0.1537	0.79
3	254	2	18.10	6.61	36.52	0.1033	0.57	0.0615	0.34	0.0816	0.45	0.1045	0.58
3	254	2	18.08	6.13	33.90	0.0927	0.51	0.0632	0.35	0.1112	0.62	0.1586	0.88
3	254	2	18.08	6.80	37.61	0.0953	0.53	0.0680	0.38	0.1103	0.61	0.1258	0.70
3	254	2	17.82	6.70	37.60	0.0960	0.54	0.0650	0.36	0.1500	0.84	0.1531	0.86
3	255	1	26.08	9.40	36.04	0.1475	0.57	0.0971	0.37	0.3870	1.48	0.1855	0.71
3	255	1	21.18	7.33	34.61	0.1070	0.50	0.0741	0.35	0.2220	1.05	0.1260	0.59
3	255	2	18.72	6.37	34.03	0.0867	0.46	0.0640	0.34	0.0527	0.28	0.0786	0.42
3	255	2	18.30	6.51	35.57	0.0926	0.51	0.0664	0.36	0.0701	0.38	0.0617	0.34
3	255	2	19.19	6.60	34.39	0.1039	0.54	0.0723	0.38	0.0986	0.51	0.1080	0.56
3	255	2	17.18	5.98	34.81	0.0917	0.53	0.0559	0.33	0.1640	0.95	0.0933	0.54
3	255	2	19.20	6.79	35.36	0.1087	0.57	0.0714	0.37	0.0520	0.27	0.0590	0.31

The data were the body weights and carcass characteristics of offspring at 8 wks of age. Numerical treatment numbers from 1 to 4 represent control, rMyo, Myo-1 and Myo-2 respectively. Sex; 1, male and 2, female. Gastrocnemius, triceps, visceral fat and back fat percentages are relative to body weight. Visceral fat was either epididymal or perametrial based on sex.